**Naia Gandiaga
Perez de Albeniz**

Compósitos Luminescentes Baseados em Celulose Bacteriana e Lantanídeos

Luminescent Composites Based on Bacterial Celullose and Lanthanides

Universidade de Aveiro Departamento de Química

2013

Naia Gandiaga
Perez de Albeniz

Compósitos Luminescentes Baseados em Celulose Bacteriana e Lantanídeos

Luminescent Composites Based on Bacterial Celullose and Lanthanides

This thesis presented to the University of Aveiro for compliance with requirements for the degree of Master in Chemistry, carried out under the scientific guidance of Dr Carmen Freire, Principal research in CICECO, University of Aveiro and of Dr. Luis Carlos Associate Professor with Aggregation Department of Physics, University of Aveiro.

.

O juri

Carlos Miguel Cardeal Enes Granadeiro

Investigador Pós-Doc da Facultade de Ciências da Universidade do Oporto

Artur Manuel Soares da Silva

Professor catedrático do Departamento de Química da Universidade de Aveiro

Prof. Doutora Carmen Sofia da Rocha Freire Barros

Investigadora principal do Centro de Investigação em Materiais Cerâmicos e Compósitos (CICECO), da Universidade de Aveiro

Agradecimentos

Aproveito esta oportunidade para agradecer a todos aqueles que tornaram possível a realização deste trabalho:

À Doutora Carmen Freire, pela ajuda, paciência, compreensão. Sem a sua orientação este trabalho não tinha sido possível realizar.

Ao Doutor Luís Carlos pela orientação e ajuda com as questões físicas.

Ao Doutor Armando Silvestre pela ajuda tanto como neste projeto como meu coordenador Erasmus.

Ao Fabio Gomes, à Carina Carvalho, ao Nuno Silva e ao Ricardo Pinto pela disponibilidade e ajuda no laboratório sempre que precisava.

Ao programa Erasmus pela oportunidade de vir a Aveiro e experimentar novas formas trabalhar num projeto.

À minha família e amigos pelo carinho, motivação e paciência sem os quais a realização deste trabalho não teria sido possível.

Este trabalho esta especialmente dedicado a os meus avos, que tiveram gostado de ver como tinha acabado o meu curso.

palavras-chave   Celulose, celulose bacteriana, acetato de celulose, nanocompósitos, filmes, lantánideos, luminescência.

Resumo   O desenvolvimento de materiais inovadores baseados em biomassa tem ganho uma atenção considerável durantes as últimas décadas devido à crescente consciencialização da sociedade em relação às questões ambientais e de desenvolvimento sustentável. A celulose é o polímero natural mais abundante e, por conseguinte, representa uma das matérias primas provenientes de fontes renováveis mais relevantes. Por exemplo, a combinação de polímeros naturais, como a celulose, com compostos inorgânicos com propriedades específicas é uma estratégia interessante e versátil para a criação de novos materiais funcionais.

Neste contexto, o objetivo deste trabalho foi preparar e caracterizar novos filmes híbridos orgânico-inorgânicos luminescentes obtidos pela combinação de acetato de celulose (preparado por acetilação completa de nanofibrilas de celulose bacteriana) e um complexo ß-dicetona de lantanídeo ($Tb(acac)_3$). Todos os filmes obtidos eram bastantes homogéneos e transparentes e demonstraram propriedades mecânicas e térmicas melhoradas, em comparação com os filmes de acetato de celulose não dopados. A análise de fotoluminescência confirmou a elevada capacidade dos lantanídeos para proporcionar propriedades de luminescência quando combinados com outros materiais. Finalmente, a adição de nanofibrilas de celulose bacteriana parcialmente acetiladas aos filmes melhorou as suas propriedades mecânicas sem afectar extensivamente a sua transparência e luminescência.

Abstract

The development of innovative bio-based materials has gained considerable attention during the last decades because of the increasing society awareness regarding environmental issues and sustainable development. Cellulose is the most abundant natural polymer and therefore represents one of the most relevant raw materials from renewable resources. For example, the combination of natural polymers, as cellulose, with inorganic compounds with specific properties is a quite interesting and versatile strategy for the design of novel functional materials.

In this context, the aim of this work was to prepare and characterize novel luminescent organic-inorganic hybrid films obtained by combination of cellulose acetate (prepared by almost complete acetylation bacterial cellulose nanofibrils) and a lanthanide ß-diketone complex (Tb(acac)$_3$). All the obtained films were very homogeneous and transparent and displayed improved thermal and mechanical properties, in comparison with the undoped cellulose acetate films. The photoluminescence analysis confirmed the high ability of lanthanides to provide luminescence properties to different materials. Finally, the addition of partially acetylated bacterial cellulose nanofibrils to the films improved the mechanical properties without affecting the transparency and luminescence in a great extent.

Index

Figure list

Tables List

Abbreviations

AGU – Anhydroglucopyranose unit

BC – Bacterial Cellulose

BCA – Bacterial Cellulose Acetate

CA – Cellulose Acetate

CDA – Cellulose Diacetate

CTA – Cellulose Triacetate

DS – Degree of Substitution

E_{em} – Emission energy

E_{ex} – Excitation energy

FTIR – Fourier Transform Infrared Spectroscopy

IUPAC –International Union of Pure and Applied Chemistry

LCD – Liquid Crystal Display

LED – Light Emitting Diode

Ln – Lanthanide

MRI – Magnetic Resonance Imaging

moleq. – mol equivalent

NIR – Near Infrared Spectroscopy

NMR –Nuclear Magnetic Resonance

OIH – Organic-Inorganic Hybrids

TGA – Thermal Gravimetric Analysis

UC – Upconversion

UV – Ultra Violet Spectroscopy

YAG – Yttrium Aluminum Garnet

λ_{em} – Emission Wavelength

λ_{ex} – Excitation Wavelength

1. The context

The interest on cellulose, as the basis for the development of new sustainable materials, increased dramatically during the last few years due to its natural abundance, with about $1,5 \times 10^{12}$ tons produced each year, renewability and specific properties.[1][2]

Apart from plant cellulose, other cellulose forms, specifically bacterial cellulose (BC) produced by several bacteria of the genus *Gluconacetobacter, Agrobacter* etc., had attracted considerable attention because of its unique properties such as, high mechanical performance, high purity, crystallinity and water holding capacity.[3][4]

The incorporation of inorganic nanoparticles with specific optical, electronic or magnetic properties into biopolymer matrices, as cellulose, represents a very interesting and promising strategy for the development of innovative biobased materials. For example, lanthanides (Ln) have been extensively used in high-performance luminescent devices, magnets, catalysts, and other functional materials because of their electronic, optical, and chemical characteristics resulting from the $4f$ electronic shells.[5][6][7]

The unique ability of lanthanide ions to emit luminescence has provided for their extensive application in laser techniques as transformers of light energy, phosphors, etc. For more than three decades, lanthanide complex compounds have also been used for the express and sensitive determination of elements in various materials, namely as shift reagents in NMR spectroscopy, for luminescence labels in immunofluorescence assays, etc.[8]

Cellulose acetate (CA) is one of the most relevant cellulose derivatives and its main applications are in the production of membranes, films, fibers, plastics and filters.[9] Only a few reports were found in the literature about the combination of cellulose acetate with luminescent compounds and were used as hydrogel film sensors or for production of nanofibers for inclusion of drugs and biomolecules modulating their fluorescence and extending their applications to biosensing, imaging and drug delivery, for instance.[10][11]

In this context, the aim of the present work is to prepare and characterize luminescent transparent films based on bacterial cellulose acetates and the lanthanide complex, terbium acetylacetonate hydrate (Tb(acac)$_3 \cdot$3H$_2$O). The work involved the

homogeneous (and partial) acetylation of BC nanofibrils, the preparation of the doped films by solvent casting and their characterization in terms of structure, morphology, mechanical properties, thermal stability and luminescent properties.

2. Introduction

2.1. Cellulose

Humans started to employ cellulose based materials for tools, for example, in Palaeolithic era for primitive utensils and in Neolithic era for light ploughs without wheels, and of course for buildings, bridges, ships, paper and much more. Moreover, for more than 1000 years, flax and cotton, where cotton is almost pure cellulose, have been used as textile fibers.[12]

However, only in the second quarter of the 19th century, cellulose became recognized as a chemical compound. In 1830, the French chemist Anselme Payen has isolated this compound from plant matter and named it as cellulose. It took some time (until the 1930s) before the molecular structure of cellulose was first established.[12][13]

2.1.1. Cellulose structure and composition

Cellulose is the main component of most plants accounting for 40-60% of dry wood, 70-80% of flax and more than 90% of raw cotton (99.9% of purified cotton). Plants such as forest trees and cotton plants synthesize cellulose from glucose produced in the cells by photosynthesis. However, some algae, bacteria and protozoans are also able to produce cellulose.[13][14][15]

Cellulose is a linear homopolymer composed of 1$\rightarrow$4 linked β-D-anhydro-glucopyranose units (AGU); the *anhydro* term arises from the elimination of a water molecule upon formation of the glycosidic bond. A typical plant cellulose chain is composed of 13000 to 14000 anhydroglucose units.[16][17]

There are three free hydroxyl groups located in the 2, 3 and 6 positions of each anhydroglucose unit, which are able to undergo the typical reactions of hydroxyl groups, for instance esterification, etherification or oxidation. These groups are therefore responsible for the chemical reactivity of cellulose. In other words, as a

carbohydrate, the chemistry of cellulose is primarily the chemistry of alcohols and it forms many of the their common derivatives.[18][19]

The anhydroglucopyranose units are in the $^4C_1$ chair conformation, which means that the –CH$_2$OH and –OH groups as well as glycosidic bonds are all in equatorial position, with respect to the mean plane of each ring (Figure 1).[15][20]
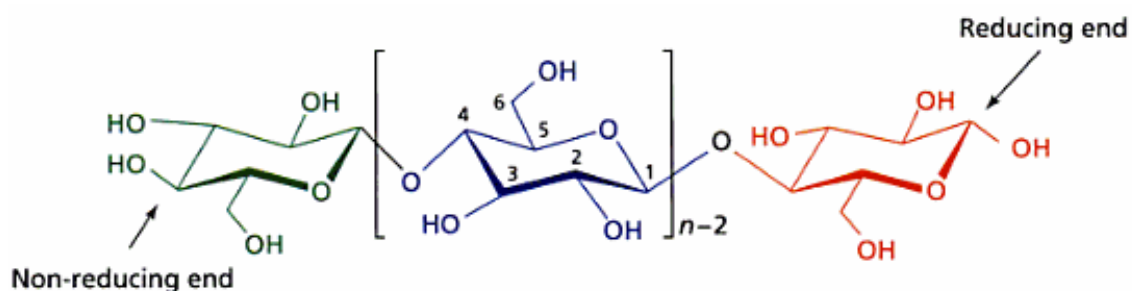
Figure 1. Molecular structure of cellulose, showing the reducing and non-reducing ends.[15]

Cellulose shows a strong tendency to form intra- and intermolecular hydrogen bonds. Intramolecular hydrogen bonding between adjacent anhydroglucose units enhances the linear integrity of the polymer chain and affects the reactivity of the hydroxyl groups, particularly of those at the C3 positions, which hydrogen bonds strongly to the pyranic oxygen of the adjacent anhydroglucose unit. The intermolecular hydrogen bonding in cellulose is responsible for the sheet-like nature of the native polymer and its insolubility in common organic solvents and infusibility (degrades before melting).

2.1.2. Cellulose fibers

The elementary structures of cellulose fibers are called elementary fibrils. These contain 36 elementary cellulose chains bound together by hydrogen bonds and that further aggregate to form microfibrils, long threadlike bundles of molecules joined by hydrogen bonds. Microfibrils aggregate further to form cellulose fibres (Figure 2).[21]
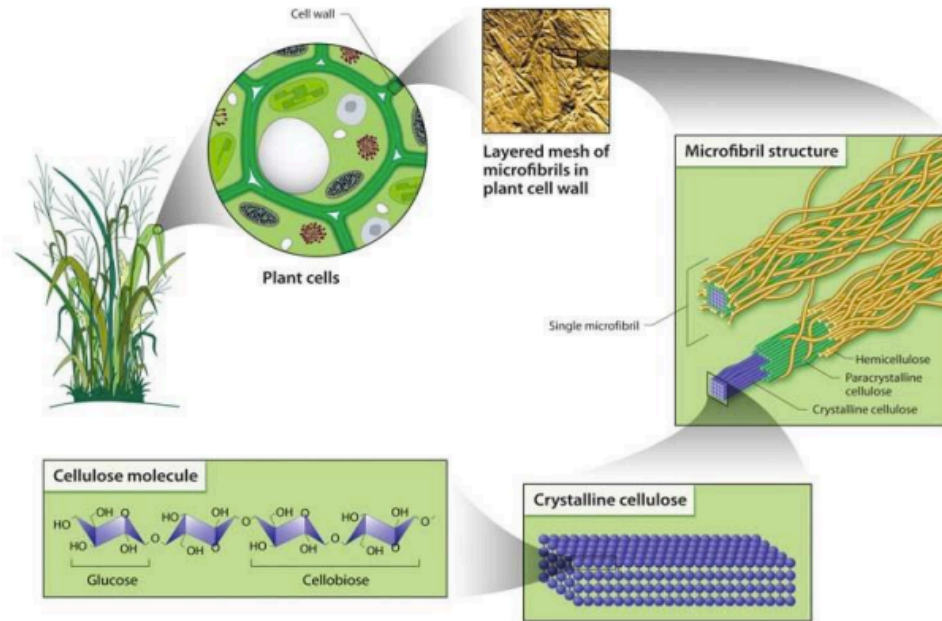
Figure 2. Cellulose structure from plant cell to molecular structure.[22]

The formation of intra- and intermolecular hydrogen bonds results in a highly crystalline structure of cellulose, with 55-70% crystalline regions, commonly designated as the degree of crystallinity, in most plants. The degree of crystallinity plays an important role in the chemical reactivity of cellulose and on its mechanical performance and chemical stability, and strongly depends on the origin and processing of the materials. In addition to the crystalline phases, native fibres contain also disordered amorphous domains (Figure 3).[20][23][24]
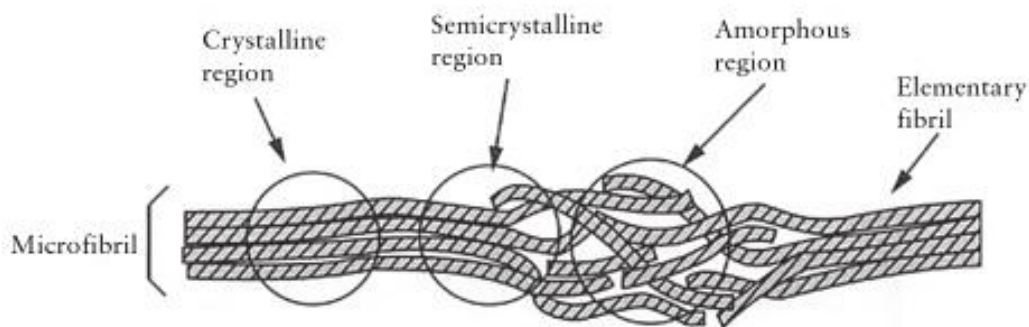
Figure 3. Crystalline and amorphous regions of cellulose microfibrils.[25]

Plant cellulose microfibrils can be regarded as innovative bio-based fibers with uniform widths, high crystallinity and high aspect ratios, originally present in the plant cell walls. Many researchers have been extensively studying the extraction of nanofibers

from wood and other plant fibers. These plant-based cellulose nanofibres, have a high reinforcing potential in composite materials because of their high tensile strength, high stiffness and high flexibility and good dynamic mechanical, electrical and thermal properties; but also because of their sustainability, easy availability as compared with other commercial fibres. However, the characteristics of cellulose fibers are altered by ageing and degradation, which is manifested in many different ways; for example, fibres are more vulnerable to light, and can weaken and change colour.[26][27]

2.1.3. Bacterial cellulose

Bacterial cellulose (BC) has attracted considerable attention in recent years because of its unique physical properties. BC is produced by several bacteria of the genus *Gluconacetobacter* (formerly *Acetobacter*), *Rhizobium, Sarcina, Agrobacterium, Alcaligenes*, etc. However, *Gluconacetobacter xylinus* (also called as *Acetobacter xylinum)* is the most studied strain, because of its efficiency to produce cellulose.[3][28]

Brown reported the production of cellulose from *Gluconacetobacter xylinum* for the first time[29]. He observed that the resting cells of *G. xylinum* produced cellulose in the presence of oxygen and glucose. These microorganisms are usually found in fruit, vegetables, vinegar and alcoholic beverages. They convert various carbon sources, such as hexoses, glycerol, dihydroxyacetone, pyruvate, and dicarboxylic acids, into cellulose, with about 50 % efficiency.[3][30]

Research on BC revealed that it is chemically identical to plant cellulose, but its morphology and properties differ from the latter. Bacterial cellulose presents a unique 3D nanofibrilar structure (Figure 4) that is responsible for most of its properties, such as high water holding capacity, porosity and remarkable mechanical properties, in both dry and wet states, for example its Young's modulus is 138 GPa, (cottons Young's modulus is between 5,5-12,6 GPa) and its tensile strength is estimated to be at least 2 GPa, (while for cotton it is around 0,3–0,6 GPa). Bacterial cellulose shows also good moldability, biodegradability and excellent biological affinity. BC has normally high degree of polymerization, but some researchers have demonstrated that different carbon sources could influence the degree of polymerization (DP), usually between 2000 and

6000, but in some cases reaching even 16000 or 20000, whereas the average DP of plant cellulose varies from 13000 to 14000.[3][30][17][31][32][33]
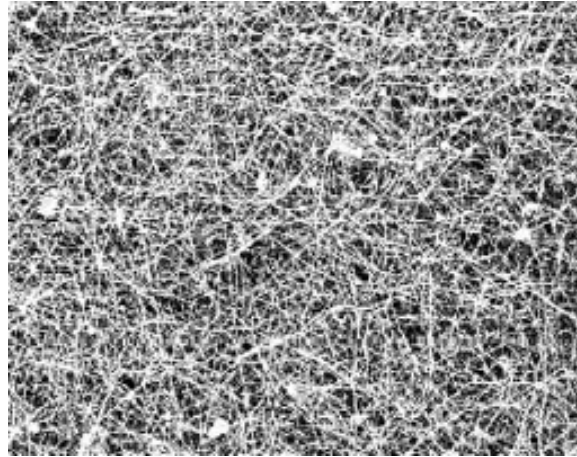
Figure 4. 3D Nano and microfibrillar structure of bacterial cellulose produced by *G. xylinum*.[3]

Bacterial cellulose is a natural hydrogel, whose properties are better than those of many hydrogels produced from synthetic polymers; for example, it displays high water content (98–99), purity and mechanical strength that are important properties for pharmaceutical and biomedical applications. Upon complete removal of water by air-drying, bacterial cellulose will only rehydrate up to 6%, because of the collapse of its tridimensional structure and establishment of strong hydrogen bonds. Through a stepwise exchange of water by other solvents, it is possible to replace water by methanol, acetone, or n-hexane, for example, while maintaining the hollow space and network structure.[34][35]

Bacterial cellulose has long been produced and used as *nata de coco*, a chewy, translucent, jelly-like food original from Philippines and produced by the fermentation of coconut water (Figure 5a). However, over the past few years, there has been an increased interest in commercial applications of bacterial cellulose. Important examples include, papermaking, electronic paper and optical and transparent nanocomposites. For example, BC based nanocomposites are not only highly transparent, but also exhibit a low thermal expansion coefficient comparable to the silicon crystal, and the mechanical strength is five times that of engineered plastics. BC has also been extensively explored in the biomedical field, such as medical pads and artificial skin (used in the therapy of

7

burns, ulcers as temporary artificial skin (Figure 5b); line of products like Biofill[®], Bioprocess[®], and Gengiflex[®]). For example, Biofill[®] is used in cases of second and third degree burns and ulcers and its efficacy has been proven in over 300 cases. Biofill[®] allows the use of antibiotic, reduces the risk of infection and the high absorption by the patient prevents dehydration, the main risk for burns. Gengiflex[®] was developed for recovering periodontal tissues.[34][36][37]

All these activities are also accompanied by the isolation of new bacterial strains, genetic modifications, and a wide variation of all laboratory culture parameters.[3]
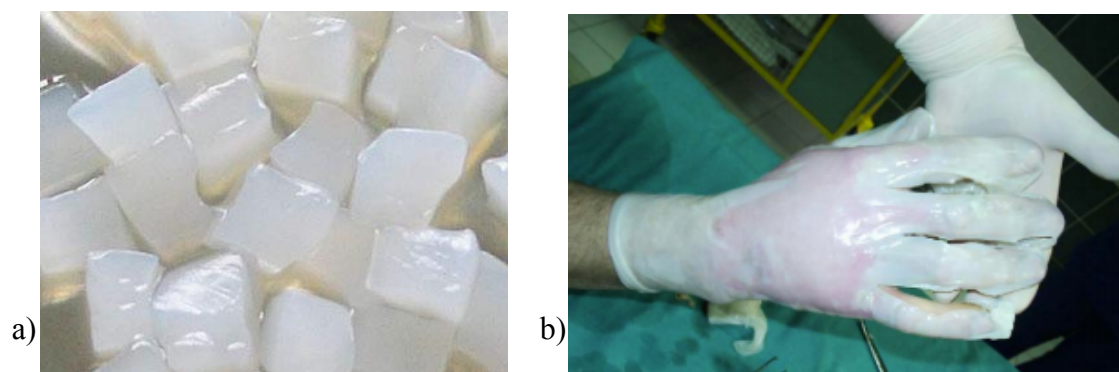
Figure 5. a) Nata de coco calorie-free food. b) BC dressing applied on a wounded hand.

2.1.4. Cellulose acetate

Paul Schützenberger prepared the first cellulose acetate in 1865 [38]. It took another 29 years before Charles Cross and Edward Bevan patented a process for its manufacture. In 1904 George Miles found that partially hydrolysed cellulose acetate dissolve in acetone. Brothers Henry and Camille Dreyfus exploited this fact to make cellulose acetate films and lacquers in 1910. During the first World War, this technology was used for waterproofing and stiffening the fabrics covering the aeroplane wings.[39]

Cellulose triacetate is manufactured by three processes among which the solution process is the most common. In this method, CA is obtained by reaction of cellulose with acetic anhydride and acetic acid in the presence of sulphuric acid. The reaction is allowed to proceed for the time needed to esterify almost all the hydroxyl groups (Figure 6). The solvent process is the second most common process, in which acetic

acid is partially or totally replaced by dichloromethane that serves as solvent for the triacetate formed. The heterogeneous process is the third method, where instead of a solvent, a non-solvent for triacetate, for instance a hydrocarbon, is added to the reaction media. When added in the correct amount, the non-solvent will prevent the dissolution of the cellulose ester and, at the end of the acetylation the cellulose derivative is found in fibrous form.[40]

The solubility of cellulose acetates depends, among other variables, on the degree of substitution; a cellulose acetate with DS of 2 − 2.5 is soluble e.g. in acetone, dioxane and methyl acetate and derivatives with higher DS are soluble in dichloromethane.[22][41]
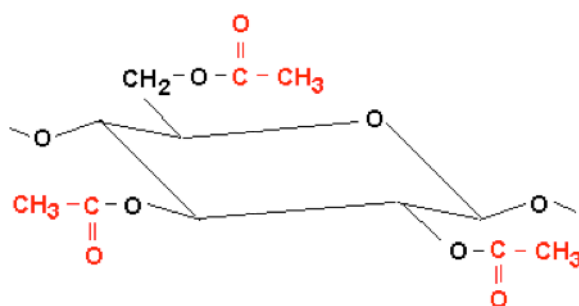
Figure 6. The structure of cellulose triacetate.[42]

The term cellulose triacetate (CTA), or simply triacetate, may be used as a generic description when at least 92% of the hydroxyl groups are acetylated. The secondary cellulose acetate, also known as diacetate or simply acetate, is readily soluble in acetone. Cellulose triacetates and diacetates can be easily converted into fibres and films with several applications.[15][41] For example, cellulose diacetate fibers are used in different kind of clothing, home furnishing or in high absorbency products, for example, feminine hygiene products, surgical products and filters. Triacetate films, instead, are used, for example, as polarizer films for LCD screens, specialized overhead projector transparencies and photographic films, motion picture films for production of animation celluloids, and packaging. As a curiosity, it is know that in cigarette filters, cellulose acetate filters are the unique which meet the requirements of filtering efficiency and taste quality and that the original Lego bricks were made of cellulose acetate.[15]

9

In what concerns the material properties, CTA exhibits good mechanical properties (for instance, better thermal stability and tensile strength than cellulose diacetate (62 MPa of tensile strength and 4% elongation, in front of 88 MPa of tensile strength and 10% elongation of CTA)) and stability under atmospheric conditions, such as water resistance. CTA is a hydrophilic polymer; it can absorb water strongly at ambient temperature. Even if CTA has been kept in vacuum for a long time, some residual water is still captured tightly by the hydroxyl groups.[43][44]

The degree of substitution of cellulose acetates plays also an important role on their biodegradability profile. The time necessary to biodegrade a cellulose acetate increases with the DS. In fact, it seems that the DS value is the predominant factor that controls the biodegradability of cellulose acetates, rather than the crystallinity.[45][46][47]

2.2. Lanthanides

2.2.1. Physical and chemical properties

The 4f-block elements are also called lanthanides, lathanones or rare earths. As defined by IUPAC, rare earth elements are the fifteen lanthanides plus scandium and yttrium. These last two elements are considered rare earth elements since they tend to occur in the same mineral deposits as the lanthanides and exhibit similar chemical properties. The name rare earth was given to them because they were originally extracted from oxides for which ancient name was earth and which were considered to be rare. The name lanthanide has been derived from lanthanum, which is the prototype of lanthanides.[48][49]

The neutral lanthanides possess the common features of a xenon structure of electrons ($1s^2\ 2s^2\ 2p^6\ 3s^2\ 3p^6\ 3d^{10}\ 4s^2\ 4p^6\ 5s^2\ 5p^6$) with two or more outer electrons ($6s^2$ or $5d\ 6s^2$) besides 4f electrons. Lanthanides find a strong dominance of the +3 oxidation state, but other oxidation states are known, although they are less stable than the +3 state. The existence of the oxidation state of +2 and +4 can be understood from the added stability associated with and empty, half-filled or filled f shell. [50]

With the exception of La^{3+} and Lu^{3+}, all Ln^{3+} ions are luminescent and their f-f emission lines cover entire spectrum, from UV (Gd^{3+}) to visible (Pr^{3+}, Sm^{3+}, Eu^{3+}, Tb^{3+}, Dy^{3+}, Tm^{3+}) and near-infrared (Pr^{3+}, Nd^{3+}, Ho^{3+}, Er^{3+}, Yb^{3+}) ranges. Some ions are fluorescent ($\Delta S=0$), others are phosphorescent ($\Delta S \neq 0$), and some are both. The transitions between the energy levels of the 4f orbital are responsible for the interesting photophysical properties of the lanthanide ions, such as the long-lived luminescence (excited state lifetime in the micro to millisecond range) (Figure 7) and the atomic-like absorption and emission lines. The 4f electrons are indeed inner electrons and the 4f orbital is shielded from the interaction with the surroundings (called Ligand-field interaction) by the filled $5s^2$ and $5p^6$ orbitals. Although weak, the influence of the host on the optical transitions within the $4f^n$ configuration is essential to explain those interesting spectroscopic features.[48][51][52]

Despite lanthanide complexes being characterized by highly efficient light emission under UV excitation (some of them even exhibit laser action in solution), their low thermal and photochemical stability and the poor mechanical properties are important disadvantages concerning their technological applicability as tuneable solid-state lasers or phosphor devices. Moreover, most of these complexes are usually isolated as hydrates in which two or three water molecules are included in the first coordination sphere of the central ion, which quenches emission due to activation of nonradiative decay path. [51]
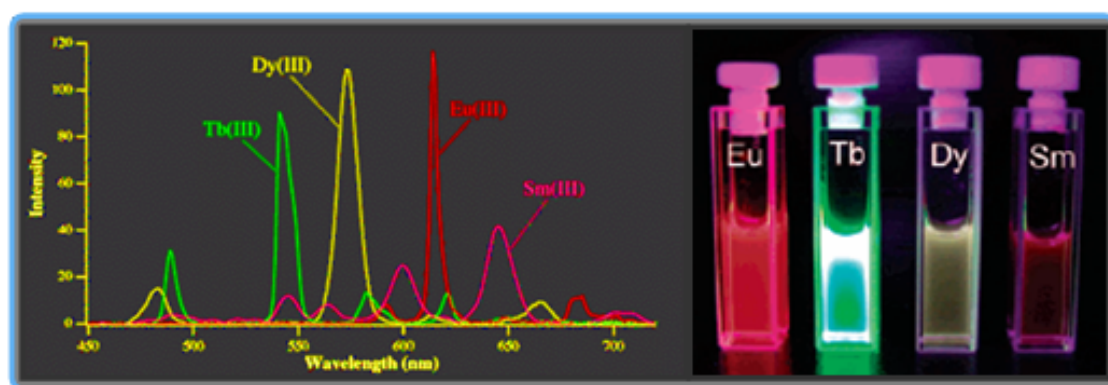
Figure 7. Emission spectra of luminescent lanthanide complexes and the colour observed of selected lanthanide (III) complexes, excited at 355 nm.[7]

If one succeeds in introducing lanthanide ions into a particular material, be it a crystal, a glass, a liquid, or a molecular material such as polymers, this material will become luminescent. A lot of work on luminescent materials based on lanthanide ions has been developed aiming to find ways to introduce lanthanides into different materials while keeping the ions brightly luminescent and the materials intact. [53]

With a simple incorporation of lanthanide ions in silica-based matrices, the obtained organic-inorganic hybrids exhibit improved luminescence properties, compared to the isolated metal salts or complexes, essentially due to the following factors:

-Better dispersion of the incorporated lanthanide ions within the matrix avoiding clustering and allowing larger concentrations of emitting centers.

-The protection from quenching effects cased by residual water, silanol groups and dopant clustering, thus decreasing the nonradiative decay pathway.[54]

Table 1. Emission characteristics of various lanthanide and their chelates.[55]

Lanthanide	Principal emission band (nm)	Transition	Typical lifetime	Detectability (mol/L)
Samarium(III)	643/598	$^5G_{5/2} \rightarrow {}^6H_{7/2}, {}^6H_{9/2}$	50-100µs	$250 \cdot 10^{-15}$
Europium(III)	613	$^5D_0 \rightarrow {}^7F_2$	0,5-1ms	$30 \cdot 10^{-15}$
Terbium(III)	545	$^5D_4 \rightarrow {}^7F_5$	0,1-2ms	$25 \cdot 10^{-15}$
Dysprosium(III)	573	$^4F_{9/2} \rightarrow {}^6H_{13/2}$	Below 10µs	$750 \cdot 10^{-15}$

Lanthanide ions can form soluble complexes with organic ligands and such complexes hold the promise that for some photonic applications they may provide low-cost alternatives to inorganic materials.[53]

The fascination for lanthanide optical spectroscopy dates back to the 1880s, when some scientists, for instance, Sir William Crookes, LeCoq de Boisbaudran, Eugène Demarçay or George Unbain, were using luminescence as an analytical tool to study crystallization processes and to identify potential new elements. After the exploratory period, lanthanide unique optical properties were taken advantage in optical glasses, filters, and lasers. In the middle of 1970s, E. Soini and I. Hemmiliä proposed lanthanide luminescent probes for time-resolved immunoassays and this has been the starting point for the present numerous bio-applications based on the optical properties of lanthanides.[56]

2.3. Organic-inorganic hybrid materials

Hybrid materials can be broadly defined as synthetic materials containing intimately mixed organic and inorganic components. This mixture yields a synergy that imparts these materials with unique features and an array of unprecedented properties (mechanical, optical, electronic, chemical, and thermal, among others) just by careful selection of the organic and inorganic components and the appropriate choice of conditions for their joint processing.[49] In addition, the term nanocomposite is used when one of the structural units, either the organic or inorganic, is in a defined size range of 1-100 nm.

Hybrid materials or even nanotechnology is not an invention of the last decade but was developed a long time ago. In ancient times, the production of bright and colourful paint was the driving force to consistently try novel mixtures of dyes or inorganic pigments and other inorganic and organic components to form paints that were used thousands of years ago. However, it was only at the end of the 20th and the beginning of the 21st century that it was realized by scientists and nanoscience opened many perspectives for approaches to new materials. The combination of different analytical techniques gave rise to novel insights into hybrid materials and made it clear that bottom-up strategies from the molecular level towards materials design will lead to novel properties in this class of materials. Organic–inorganic hybrids (OIH) can be applied in many branches of materials chemistry because they are simple to process and are amenable to design on the molecular scale.[7] [56]

All the new hybrid materials have the common characteristic that they are prepared at moderate temperatures, lower than 100ºC. Such processes give materials where the organic matter remains associated with an inorganic skeleton, being homogeneously distributed among the whole material. However, there are significant peculiarities from one type of hybrid to another, peculiarities that depend both on the different association energy between the organic and the inorganic fractions, and on the different microstructural composition of the two parts. In consequence, the associated physical and chemical properties of different types of materials can also be quite different.[56]

Many natural materials consist of inorganic and organic building blocks distributed on the (macro)molecular or nanoscale. In most cases the inorganic part provides mechanical strength and a complete structure to the natural objects while the organic part delivers bonding between the inorganic building blocks and the soft network. Typical examples of such materials are bone, or nacre.

Organic-inorganic hybrids can be applied in many branches of materials chemistry because they are simple to process and are adaptable to design on the molecular scale. Currently there are four major topics in the synthesis of organic-inorganic materials:

- Their molecular engineering
- Their nanometer and micrometer-sized organization
- The transition from functional to multifunctional hybrids
- Their combination with bioactive components

Some examples of hybrid materials include the incorporation of inorganic nanoparticles, with specific optical properties, into organic matrices for high-tech applications and of magnetic inorganic compounds in organic polymeric matrices or the increment of the mechanical strength of polymers by using inorganic structural hybrid materials (for example scratch-resistant coatings for plastic glasses).[7][49][56]

2.4. Luminescent materials

In recent years, lanthanide-doped luminescent materials have received extensive attention for their potential applications such as phosphors and solar cells (Figure 9), flat-panel displays, solid state lasers, optical telecommunications, medical diagnostics and various other fields. Currently, the most important commercialised use of luminescent lanthanide complexes is in medical diagnostics, where they are used to detect small amounts of biomolecules that can tell about the physical condition of a patient.[53][52]

Lanthanide ions exhibit unique luminescent properties, including the ability to convert near infrared long-wavelength excitation radiation into shorter visible wavelengths through a process known as photon upconversion (UC).

Upconversion (UC) is a type of nonlinear process, capable of converting a lower energy excitation light into a higher energy emission. To understand this phenomenon, one must know the differences between a nonlinear process and the typical single photon excitation fluorescence and how UC compares with the other common nonlinear processes. In Figure 8, typical fluorophores exhibit the phenomenon of Stokes shift, in which the emission light is of a longer wavelength (λ) than the excitation source (i.e., $\lambda_{ex} < \lambda_{em}$). In terms of energy, this implies that the emission energy (E_{em}) is lower the excitation energy (E_{ex}). Additionally, since only one photon is involved in the excitation, the process can be termed as single photon (linear) excitation fluorescence. Hence, an obvious difference between this and the nonlinear processes is the number of photons involved. Nonlinear processes will involve more than one photon (illustrated as two photons in Figure 8b, but can actually involve more than two). Then, as a consequence of this multiphoton excitation, E_{ex} for the nonlinear processes is correspondingly lower than that of the emission. Correspondingly, the excitation light has a longer wavelength than the emission light.[57][58]
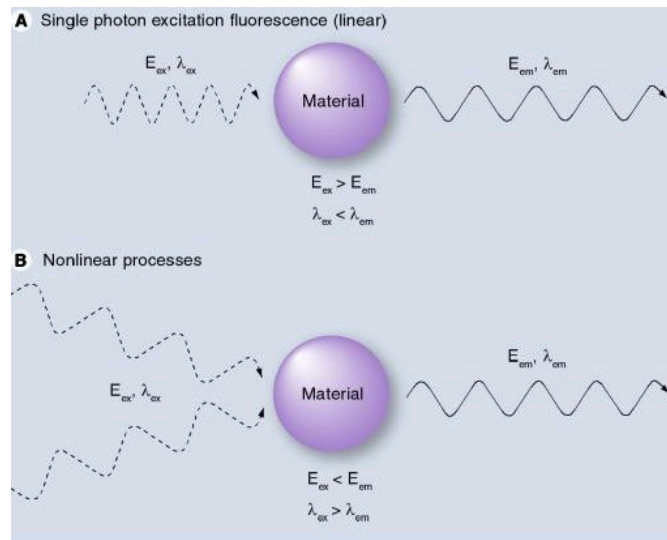
Figure 8. The main differences between a) single photon excitation fluorescence (linear) and b) nonlinear processes.

Another important component of UC nanoparticles is the host materials, which determines the optical properties and emission efficiency. The desired host materials should have close lattice matches with the dopant ions and low lattice phonon energies to minimize energy losses and maximize radiative emissions. Many host materials, as well as lanthanide dopant ions, have been used to produce UC nanoparticles with different emissions by varying host-dopant combinations. Among these lanthanide-doped UC nanoparticles, $NaYF_4$ co-doped with Yb^{3+}/Er^{3+} or Yb^{3+}/Tm^{3+} nanoparticles have been reported as the materials with the highest UC efficiency. [57]

In recent years lanthanide-doped upconversion nanocrystals have been developed as a new class of luminescent optical brighteners in paints, papers, clothing or detergent, in pharmaceuticals fields like protection products, quantum dots for applications in biological assays and medical imaging in diagnostics or photodynamic therapies. Another application areas are in emergency exit lighting, discharge lamps, in cosmetics (dental ceramics, tanning lamps), photocopiers etc. (Figure 9).[58]
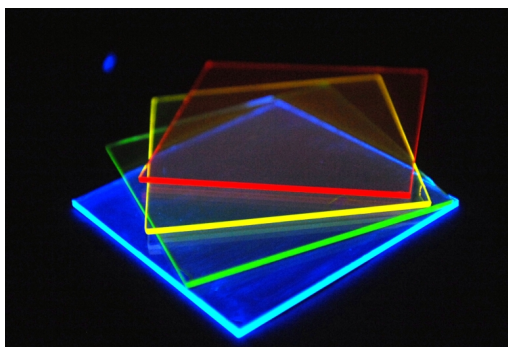
Figure 9. Organic solar concentrators collected and focused in different colours of sunlight. [59]

Terbium (Tb^{3+}) is an interesting candidate for green light emission due to the strongest luminescence at 545 nm among the $^5D_4 \rightarrow {}^7F_J$ ($J = 3,4,5,6$) transitions ranging from 380 to 630 nm resolved over the temperature range of 10-300 K in ion implanted solids, colloidal nanoparticles, xerogel films, or other hosts.[60]

Cerium (Ce^{3+}) ion is also interesting because of its strong *f–d* transition. It possesses a $4f^1 5d^0$ electronic configuration, and accordingly, the *4f–5d* transition can produce luminescence in the visible region. Particularly, because the surrounding crystalline environment can remarkably affect the *5d* energy level of Ce^{3+}, the emission wavelengths can be tuned. *Yttrium Aluminum Garnet* (YAG, $Y_3Al_5O_{12}$) doped with Ce^{3+} is probably one of the most important cerium doped materials. The first generation of commercial white Light-Emitting Diode (LED) was fabricated by mixing the InGaN chip emitting at around 460 nm (blue light) and the YAG: Ce^{3+} phosphors of yellow emitting.[61]

3. Reagents and general procedures

3.1. Reagents

Bacterial cellulose, in the form of wet membranes, was produced in our laboratory using conventional culture medium conditions.[62]

Cellulose triacetate $[C_6H_7O_2(OOCCH_3)_3]_n$ was obtained from Fluka Analytical; terbium triacetylacetonate complex, was prepared in the physics department. The complex was prepared by an addition of terbium chloride (TbCl$_3$·6H$_2$O, 99.9%, Aldrich) to acetyl acetone (99.5%, Aldrich) in an ethanol solution 1:3 molar ratio followed by the addition of sodium hydroxide until the pH reaches 6.5. The obtained complex was filtrated and dried under vacuum[63]. All other solvents and reagents were of analytical grade and used as provided by the suppliers.

3.2. Acetylation of bacterial cellulose

A lyophilized bacterial cellulose membrane was cut in small pieces and suspended in a mixture of 20 moleq. (mol equivalent) of acetic acid, 9 moleq. of acetic anhydride and 0,08 moleq. of concentrated sulphuric acid (add enough quantity until the cellulose is completely covered) at 50 ºC. After 30-40 minutes of reaction, cellulose was completely dissolved in the reaction media. The excess of acetic anhydride was destroyed by the addition of 5-10 mL of aqueous acetic acid (80%). After cooling, cellulose acetate was precipitated by carefully adding water to the reaction mixture. The product was washed with water until complete removal of acetic acid, and dried in a ventilated oven.[64]

3.3. Partial acetylation of bacterial cellulose

Bacterial cellulose membrane was disintegrated with an Ultra-Turrax equipment for 30 minutes at 2500 rpm, and then submitted to solvent exchange with ethanol and acetone. For the acetylation step, 225 mL of acetic anhydride were placed in a 500 mL round bottomed flask followed by 0,9 wt% of H$_2$SO$_4$ (0,75 mL), and finally disintegrated BC (15 g) was added under stirring. The treatment was conducted at 30 ºC for 4h. At the end of the reaction time the acetylated BC was filtered and sequentially washed with

acetone, ethanol, water and again with ethanol. Then, to remove any trace of acetic anhydride and other impurities, the modified fibers were Soxhlet extracted with ethanol for 12 hours and finally dried at 60 ºC for 24 hours.[65]

3.4. Preparation of cellulose triacetate/lanthanide films

0,5 g of cellulose acetate (synthesized BCA and commercial cellulose triacetate) were dissolved in dichloromethane (around 10-15mL) with continuous stirring, followed by the addition of different amounts of $Tb(acac)_3 \cdot 3H_2O$ (0, 1, 5 and 10% relative to the cellulose triacetate mass). Finally, films were obtained by casting in petri dishes at room temperature in a ventilated oven.

Additionally, cellulose triacetate films with 5% of $Tb(acac)_3$ and 5 and 10% of partially acetylated bacterial cellulose fiber were also prepared following the procedure described above.

4. Characterization methods

BCA, commercial cellulose triacetate and partially acetylated cellulose triacetate, were characterized by FTIR, NMR and SEM while the corresponding films doped with Tb(acac)$_3$·3H$_2$O by nuclear magnetic resonance (^{1}H NMR and ^{13}C NMR), infrared spectroscopy (FTIR-ATR), thermogravimetric analysis (TGA), mechanical assays, ultraviolet-visible spectroscopy (UV-Vis), photoluminescence and lifetime, emission quantum yields, scanning electronic microscopy (SEM), and water uptake.

4.1. Nuclear Magnetic Resonance

Cellulose triacetate were analysed by ^{1}H NMR and ^{13}C NMR using a BRUKER DRX 300 spectrometer (300,13 MHz for ^{1}H NMR and 75,47 MHz for ^{13}C NMR) in liquid-state, using 15 mg of bacterial cellulose triacetate sample mashed solid and deuterated chloroform (CDCl$_3$) as solvent.

Solid-state CP/MAS ^{13}C NMR spectra of 0%, 5% and 10% Tb(acac)$_3$·3H$_2$O doped BCA films were obtained at 12 kHz using a NMR Bruker 500 spectrometer.

4.2. Fourier Transform Infrared Spectroscopy

FTIR spectra were acquired using a Brüker IFS 55 FTIR spectrometer, with a resolution of 4 cm^{-1} after 256 scans. Spectra were collected from 4000 to 300 cm^{-1}.

4.3. Thermogravimetric Analysis

Thermal decomposition temperatures of BCA and commercial samples of 0%, 1%, 5% and 10% of Tb(acac)$_3$·3H$_2$O were determined by thermogravimetric analyses (TGA) on a Shimadzu TGA-50 analyser equipment. The assays were run under nitrogen atmosphere in the range of 20-800°C.

4.4. Mechanical Assays

The test samples were cut into rectangles of 4 cm length and 0,5 cm width, and acclimated 2 days in a dissecator to stabilize the humidity constant. All analysed measurements were performed for at least four (and maximum eight) replicates for each sample and the average value was recorded. The mechanical assays were made with an Instron 5966 mechanical testing equipment with a cross-head speed of 10 mm/min using a 1 kN static load cell.

4.5. Photoluminescence and lifetime

The photoluminescence spectra were recorded at room temperature with a modular double grating excitation spectrofluorimeter with a TRIAX 320 emission monochromator (Fluorolog-3, Horiba Scientific) coupled to a R928 Hamamatsu photomultiplier, using a front face acquisition mode. The excitation source was a 450 W Xe arc lamp. The emission spectra were corrected for detection and optical spectral response of the spectrofluorimeter and the excitation spectra were corrected for the spectral distribution of the lamp intensity using a photodiode reference detector. The emission decay curves were measured with the setup described for the luminescence spectra using a pulsed Xe–Hg lamp (6 μ s pulse at half width and 20–30 μ s tail).

$^5D_4$ lifetime values (ms) were monitored at 545 nm under distinct excitation wavelengths (λ_{ex}, nm).

4.6. Emission quantum yields

The absolute emission quantum yields were measured at room temperature using a quantum yield measurement system C9920-02 from Hamamatsu with a 150 W Xenon lamp coupled to a monochromator for wavelength discrimination, an integrating sphere as sample chamber and a multi channel analyser for signal detection. Three measurements were made for each sample so that the average value is reported. The method is accurate to within 10 %.

4.7. UV-Vis-NIR absorption spectra

UV-Vis-NIR absorption spectra were recorded at room temperature, using a dual-beam spectrometer Lambda 950, (Perkin-Elmer) with a 150 mm diameter Spectralon integrating sphere.

4.8. Scanning Electronic Microscopy

SEM micrographs were obtained with a HR-FESEM SU-70 Hitachi equipment. Samples were mounted on carbon tape and coated with carbon for SEM analysis.

4.9. Water-uptake

Films with 0%, 5% and 10% of Tb(acac)$_3$·3H$_2$O were immersed in water at room temperature to study their water uptake. The samples were taken out of water and weighed after gently drying the surface and then re-immersed in water. The measurement was carried out after one week.

5. Results and discussion

This study began with the acetylation of BC, aiming to prepare BC triacetate derivatives, following standard procedures described in the literature for plant fibres.[64]

The obtained BC acetates were characterized and then used for the preparation of transparent films doped with lanthanides.

5.1. BC acetylation

BC acetylation was carried out by reaction of BC nanofibres with acetic anhydride, in the presence of acetic acid and sulphuric acid, for 30-40 minutes at 50ºC (Figure 10).

Figure 10. Schematic representation of BC acetylation and visual aspect of BC before and after modification.

The occurrence of the acetylation reaction was primary confirmed based on the visible changes occurred after BC modification. The white lyophilized BC membranes were converted into an ivory hard shape solid (BCA).

The success of the BC acetylation was then further confirmed by FTIR and ^{1}H and ^{13}C NMR analysis.

5.1.1. Fourier Transform Infrared Spectroscopy

The FTIR spectra of BC, BCA and of commercial cellulose triacetate are shown in Figure 11.

The FTIR spectrum of pure BC is characterized by a broad band at 3500-3000 cm^{-1}, attributed to O–H stretching vibrations; at 2892 cm^{-1} associated with C–H stretching vibration of CH and CH$_2$ groups, and a sharp and steep band at around 1162 cm^{-1} due to the presence of C–O–C stretching vibration of the cellulose chains.[66] [67]

The main bands observed on the spectrum of BCA are assigned to the carbonyl C=O stretching (1730 cm^{-1}) and bands with strong intensity are also found at 1212 cm^{-1} and 1030 cm^{-1}, both corresponding to the stretching vibrations of C–O–C bonds. [68] Therefore, the success of the BC acetylation was mainly confirmed by the appearance of the intense band at around 1730 cm^{-1}, associated to the C=O stretching vibrations of the acetate groups, and by the almost complete disappearance of the hydroxyl groups vibration at around 3500-3000 cm^{-1}, as a result of the extensive acetylation of the hydroxyl groups of BC.

No significant differences between the FTIR spectra of BCA and of the commercial cellulose triacetate were observed.
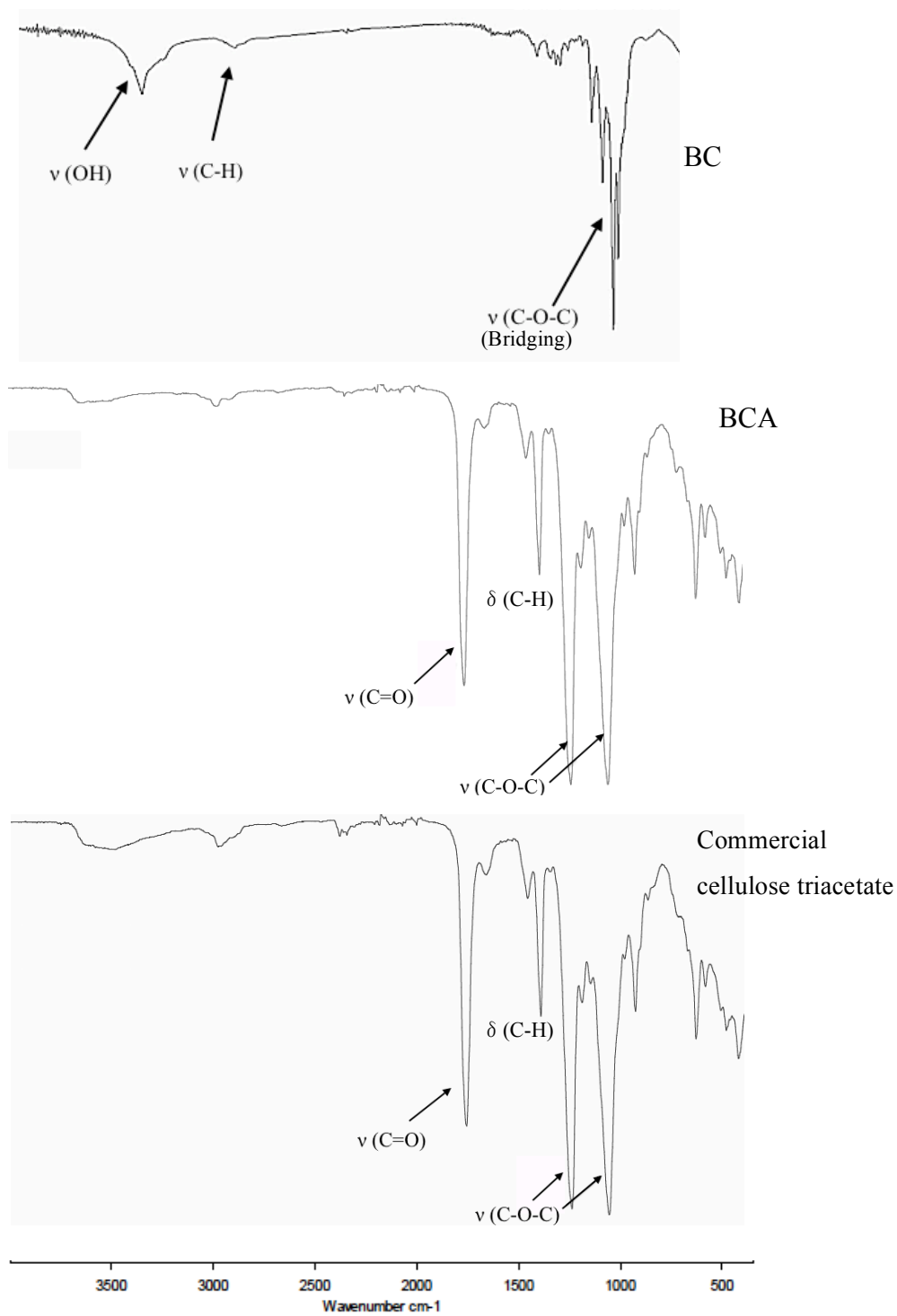
Figure 11. ATR FTIR spectra of bacterial cellulose (BC)[67], bacterial cellulose triacetate (BCA) and commercial cellulose triacetate.

5.1.2. Nuclear Magnetic Resonance

The ^{1}H-NMR and ^{13}C-NMR spectra of BCA are shown in Figure 12.

The NMR spectrum of BCA is characterized by ^{1}H resonances at δ =3,59-5,14 ppm assigned to the protons linked to glycosidic carbons (in the following order H-3,1,2,6,5,4) and resonances between 1,78 and 2,17 ppm (O=C-C$\underline{H}_3$), which is in close agreement with the values described in literature for cellulose triacetates and obtained for commercial samples (results not shown).[69][70]

The ^{13}C NMR spectrum of BCA is also in accordance with the literature, with carbon resonances at δ=170 ppm (C=O), 20 ppm (O=C-$\underline{C}$H$_3$), 100,5 ppm (C1), 61,8 ppm (C6) and 71-77 ppm (C2,3,4,5).[71][72][73]
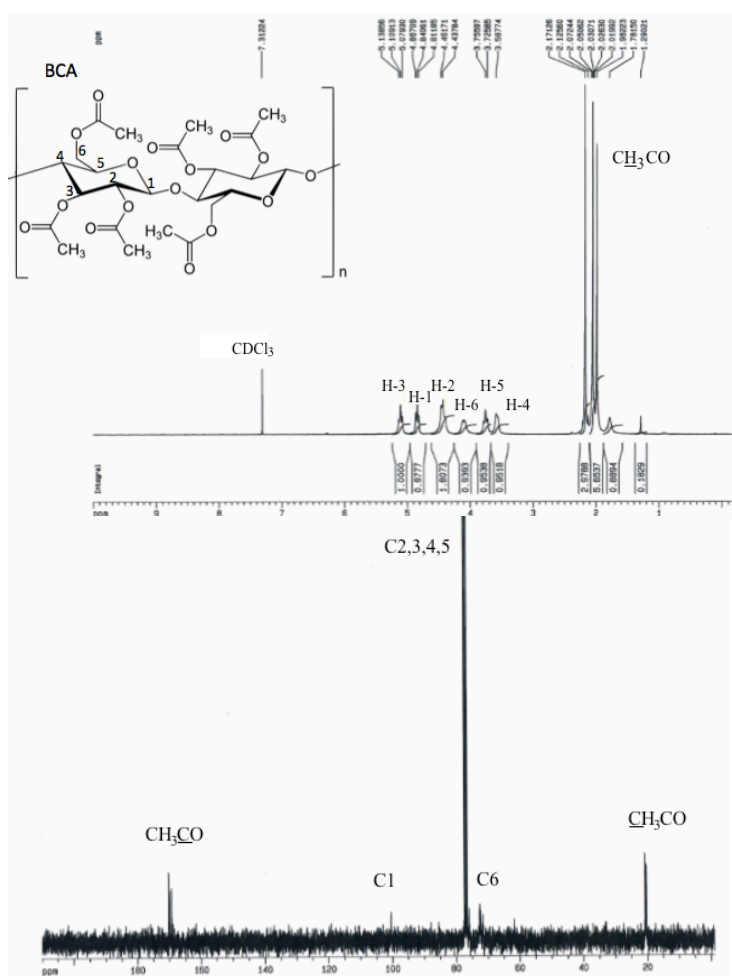
Figure 12. ^{1}H-NMR and ^{13}C-NMR (liquid state) of BCA sample.

5.1.3. Scanning Electron Microscopy

The effect of the acetylation reaction on the morphology of BC was studied by SEM. As can be observed in Figure 13 the characteristic three-dimensional network of BC was totally destroyed. These results are expectable, since almost all hydroxyl groups were acetylated and the nanofibrillar structure inevitably destroyed.
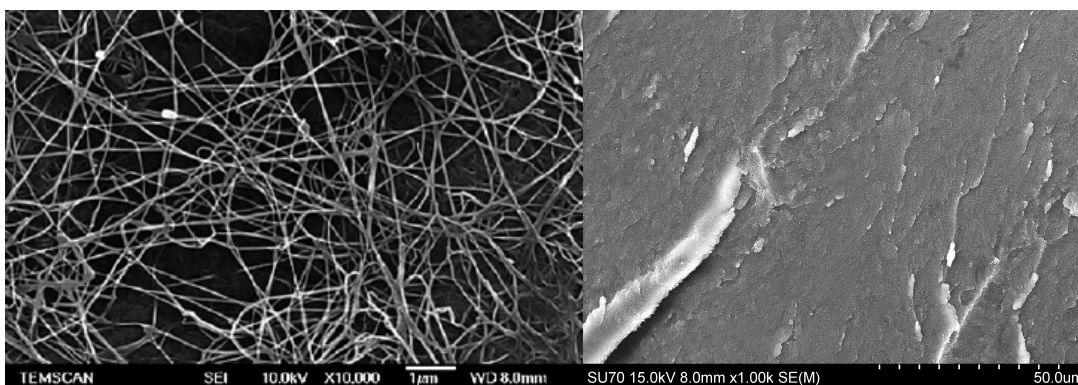
Figure 13. SEM images, pure BC membrane (left) [74] and BCA film (right).

5.2. BCA-lanthanide films characterization

The films of BCA and commercial cellulose triacetate doped with lanthanides (Figure 14) were prepared by dissolving BCA or commercial cellulose triacetate and different amounts of Tb(acac)$_3$ in dichloromethane, followed by solvent casting of the final solution.
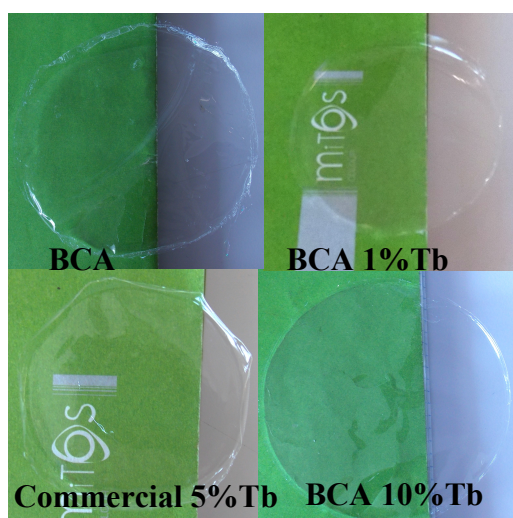
Figure 14. Transparent films from BCA and commercial cellulose triacetate doped with Tb(acac)$_3$.

As shown in Figure 14, the films obtained are very homogeneous and transparent, suggesting a good dispersion of the lanthanide inside the cellulose acetate matrices.

The BCA doped films were characterized by FTIR, NMR, TGA, mechanical assays, water-uptake and photophysical analysis.

5.2.1. Fourier Transform Infrared Spectroscopy

The FTIR spectra of all BCA (and commercial cellulose triacetate) films doped with Tb(acac)$_3$·3H$_2$O showed only the typical absorption bands of cellulose triacetate matrices described above. The characteristic vibrations of Tb(acac)$_3$ observed in the spectrum of the pure compound, were not perceptible, certainly because of the lower contents used and to some overlapping promoted by the BCA vibrations (Figure 15).
With 10% it should seeing some signals of Tb(acac)$_3$ shall be seen, although none of the characteristic bands can be distinguished.
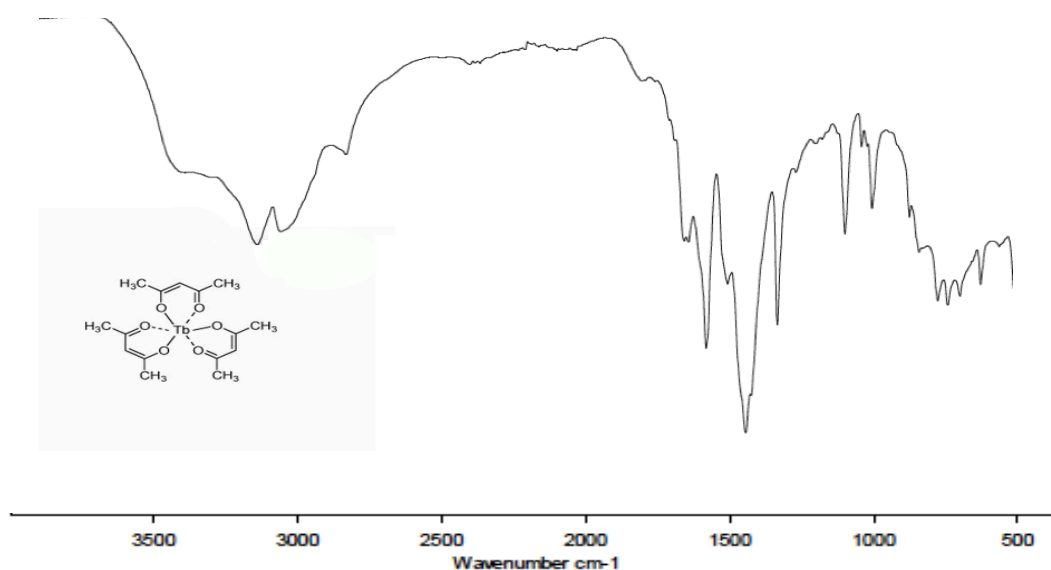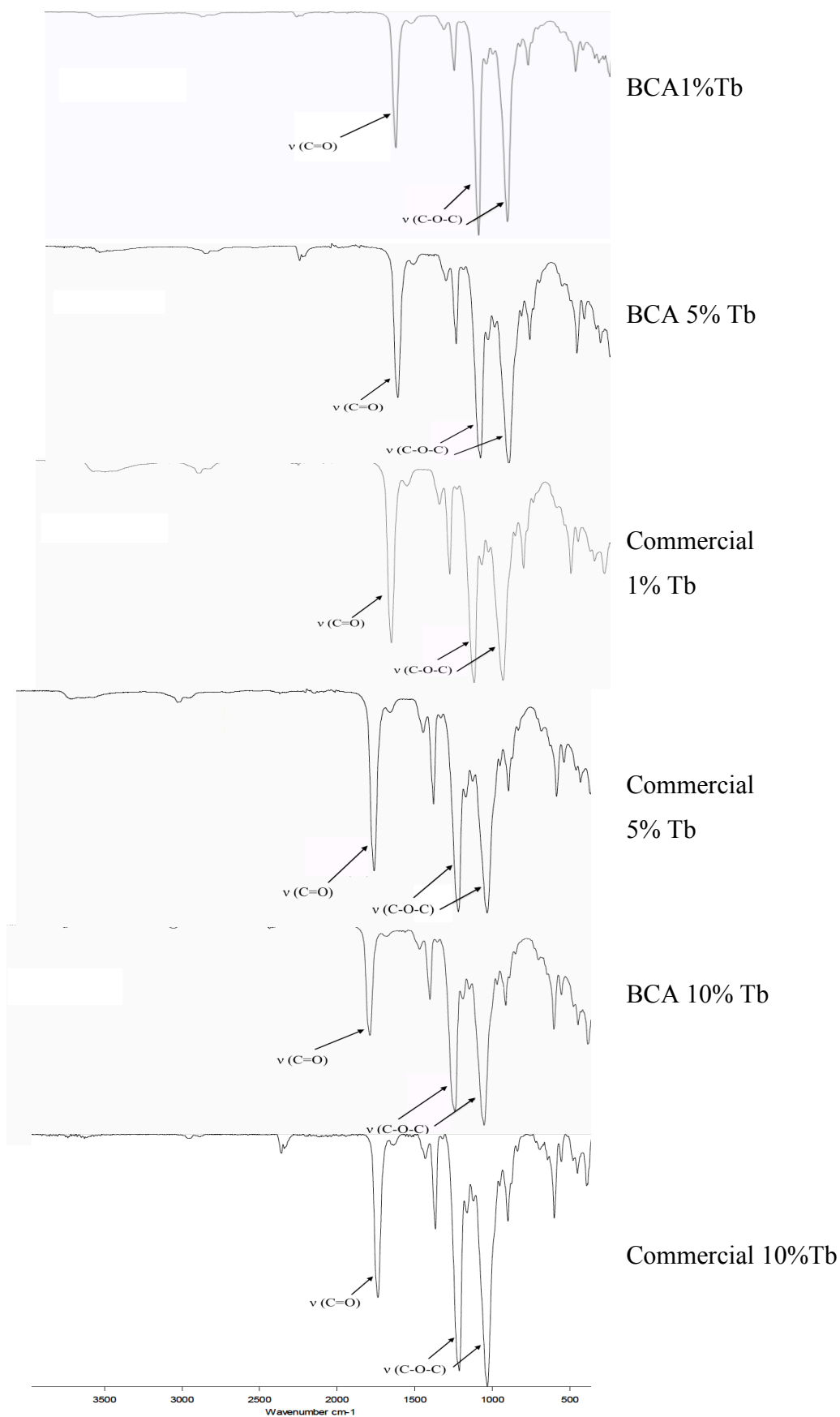
Figure 15. ATR- FTIR spectrum of Tb(acac)$_3 \cdot$3H$_2$O, BCA 1% Tb, Commercial 1% Tb, BCA 5% Tb, Commercial 5% Tb, BCA 10% Tb and Commercial 10% Tb.

5.2.2. Solid state ^{13}C NMR

The solid state CP/MAS ^{13}C-NMR spectra of BCA, BCA Tb(acac)$_3$ 5% and BCA Tb(acac)$_3$ 10% (Figure 16) were obtained to determine the potential interactions established between the lanthanide complexes and the acetate groups.

As in the FTIR spectra, the typical resonances of the lanthanide complex were not observed in the CP/MAS ^{13}C-NMR spectra of BCA Tb(acac)$_3$ 5% and BCA Tb(acac)$_3$ 10%.
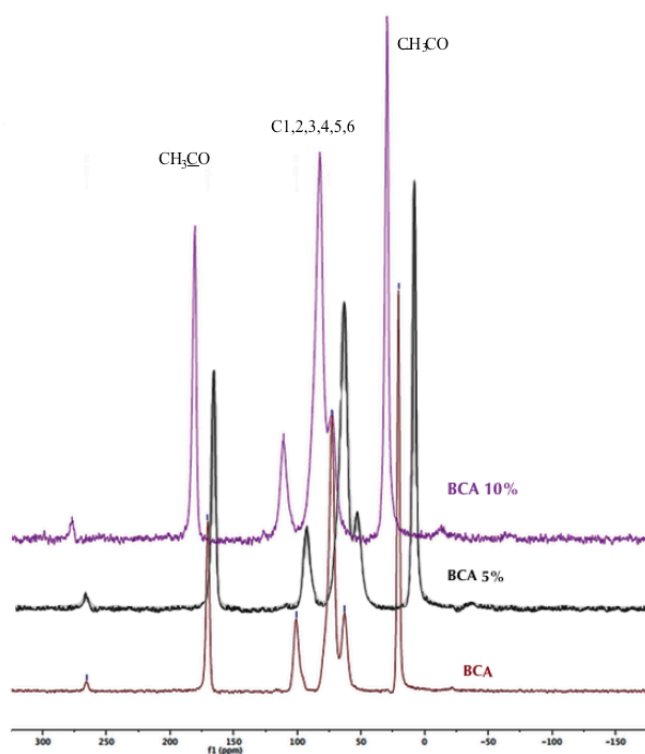
Figure 16. The solid state CP/MAS ^{13}C-NMR spectra of BCA, BCA 5% Tb, BCA 10% Tb[71]

These lanthanide complexes are paramagnetic metal complexes, which induce changes in the chemical shift of protons close to an electronegative substituent with a lone electron pair (carbonyl groups for example). The ability of certain lanthanide complexes to induce large change in chemical shifts with relatively small line broadening effects made them popular as NMR shift reagents.[76]

This is markedly seen in the proton resonances and not so likely to occur in C13 resonances. However, an interaction between BCA and the lanthanide can be observed by ^{13}C-NMR.

On the basis of the spectrum of the undoped BCA, spectrum bands whit terbium contents of 5% have a negative deviation, while the film with 10% terbium have positive deviation. This point, needing more time to his research, stays open for future work.

In Table 2, the effect of the Tb(acac)$_3$ caused in the BCA carbons are summarized.[77][12]

Table 2. Chemical shifts of ^{13}C NMR solid state for the BCA and terbium complex samples.

δ/ppm	BCA 0% Tb	BCA 5% Tb	BCA 10% Tb
C=O	170,29	170,33	170,38
C1	100,89	100,84	100,74
C2-C5	72,90	72,99	73,03
C6	62,68	62,70	62,49
C-Me	20,38	20,44	20,42

5.2.3. Thermogravimetric Analysis

Cellulose triacetates (CTA) typically degrade in two steps (Figure 17, Table 3). The first step with a maximum degradation temperature at around 330ºC represents the main degradation of the cellulose triacetate chains. The second one starts at around 476 °C and is attributed to the carbonization of the products to ash. In the case of the BCAs films prepared in this study, the maximum degradation temperature (339ºC) is very similar to that found in literature. However, the commercial cellulose triacetate films are slightly more stable, being the maximum degradation temperature 361ºC.[79][80][9]

The TGA analysis of cellulose triacetate doped with Tb(acac)$_3$ films showed no great changes on the Tdi when compared with the undoped ones. Only an increment of 9ºC was observed for the BCA film with 1% of Tb(acac)$_3$·3H$_2$O. Furthermore, it can be observed (Figure 17) that the major weight loss events occur at the same interval (310-360ºC). These results indicate that the thermal behaviour of the cellulose acetate films was poorly affected by doping with the lanthanide complex.[81][82]

Another important observation, from the TGA data, is that no significant weight loss event was observed within 150-220ºC for all cellulose triacetate films doped with the lanthanide complex precursors. This could reveal that after the doping process the water molecules coordinated to the Tb^{3+} ion are replaced by interactions between the Tb^{3+} ions and the oxygen atoms of the carbonyl groups of the cellulose triacetate chains. However, as already referred this observation can be also related with the low quantities used to prepare the films.[82]
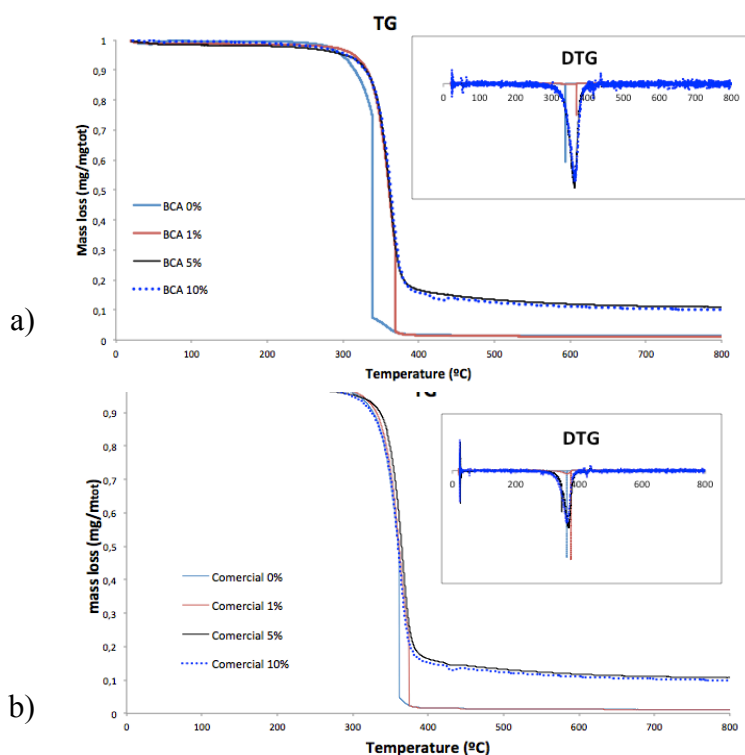
Figure 17. a) TG and DTG of BCA 0% and BCA 1% Tb, BCA 5% Tb, BCA 10% Tb b) TG and DTG of Commercial 0% and Commercial 1% Tb, Commercial 5% Tb, Commercial 10% Tb

Table 3. Thermal properties of bacterial cellulose triacetate (BCA) and commercial cellulose triacetate films with terbium complex

Sample	Tdi/ºC	Tdmax/ºC
BCA 0% Tb	288	338,58
BCA 1% Tb	297	368,81
BCA 5% Tb	277,5	363,09
BCA 10% Tb	285,5	364,11
Commercial 0% Tb	289	361,28
Commercial 1% Tb	290	374,56
Commercial 5% Tb	287	362,75
Commercial 10% Tb	285	368,43

5.2.4. Mechanical Assays

The mechanical performance of the materials was evaluated by tensile experiments. Tensile tests were performed, at room temperature, for BCA and commercial cellulose triacetate films. Figure 18 and Table 4 show the tensile mechanical properties, including Young's modulus, tensile strength and elongation at break, determined from the typical stress-strain curves.

In general, the incorporation of 1 and 5% of the lanthanide complex into the BCA matrices produced films with increased mechanical properties, as observed by increments on the elongation at break and tensile strengths, probably due to the establishment of interactions between $Tb(acac)_3$ and BCA, as confirmed by solid state ^{13}C NMR analysis (Figure 17) . This tendency is particularly visible for the films of commercial cellulose triacetate. However, the samples with 10% terbium showed a decreased in these properties when compared with the samples with 5%, probably due to the increased tendency of aggregation of $Tb(acac)_3$.[83]

Table 4. Young's modulus, tensile strength and elongation at break values of bacterial cellulose triacetate (BCA) and commercial cellulose triacetate with terbium complex.

Sample	Young Modulus (MPa)	Tensile Strength (MPa)	Elongation at Break (%)
BCA 0% Tb	5898,44±935,66	79,67±15,19	1,26±0,58
BCA 1%	5010,31±591,53	82,72±27,31	1,76±0,80
BCA 5% Tb	5455,83±227,99	112,85±12,51	3,19±1,10
BCA 10% Tb	5666,5±997,76	80,65±18,88	1,51±0,5
Commercial 0% Tb	3414,84±294,94	77,06±6,50	3,73±0,89
Commercial 1% Tb	4646,20±928,54	101,17±21,88	4,18±1,48
Commercial 5% Tb	6896,24±1023,07	162,11±28,32	8,88±2,51
Commercial 10% Tb	5843,37±917,40	145,56±26,00	11,14±2,45
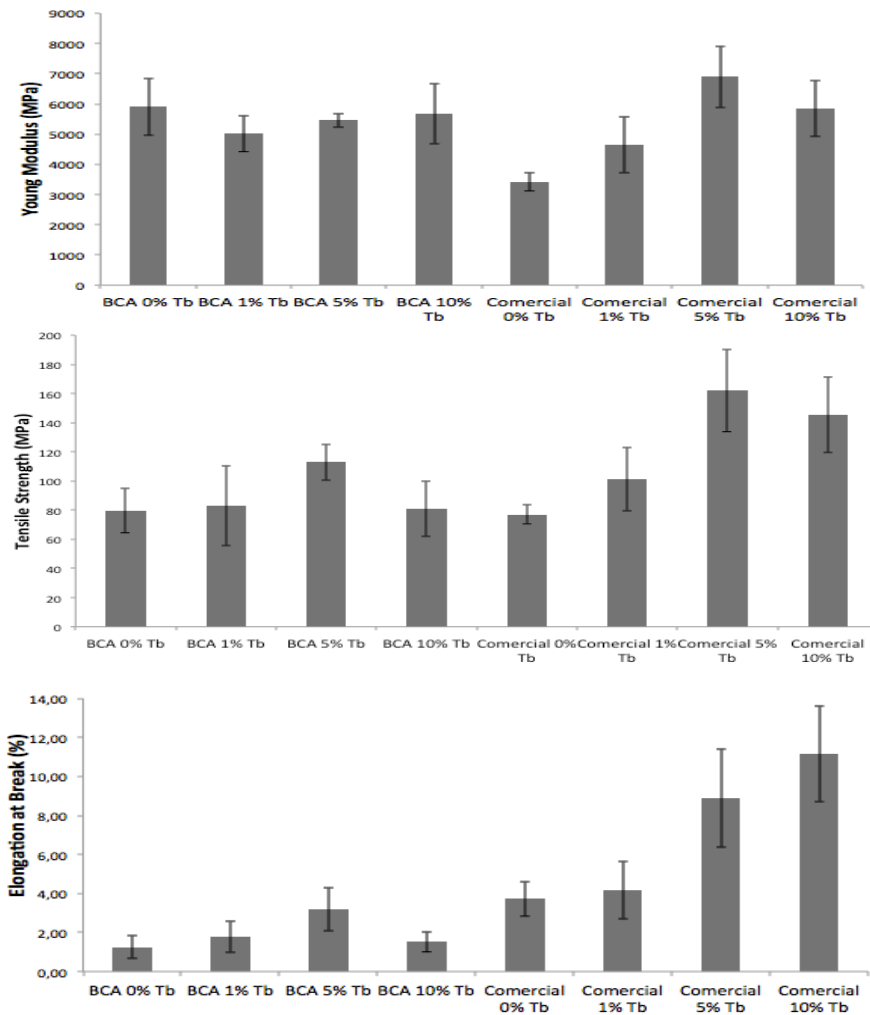
Figure 18. Young's modulus, tensile strength and elongation at break graphics of bacterial cellulose triacetate (BCA) and commercial cellulose triacetate with terbium complex.

5.2.5. Water-uptake

Swelling studies were performed for BCA and commercial cellulose triacetate films in order to evaluate their water sensitivity in a period of a week (Figure 19).

All films absorbed water in the conditions tested; however, the incorporation of the lanthanide complex decreases the water absorption capacity. The cellulose acetate groups provide a hydrophilic character to the films, and their ability to absorb some water. When incorporated in the films, the terbium complexes, could release the water molecules in the first coordination sphere, interacting with the acetate groups, and therefore reducing the water absorption.[82]
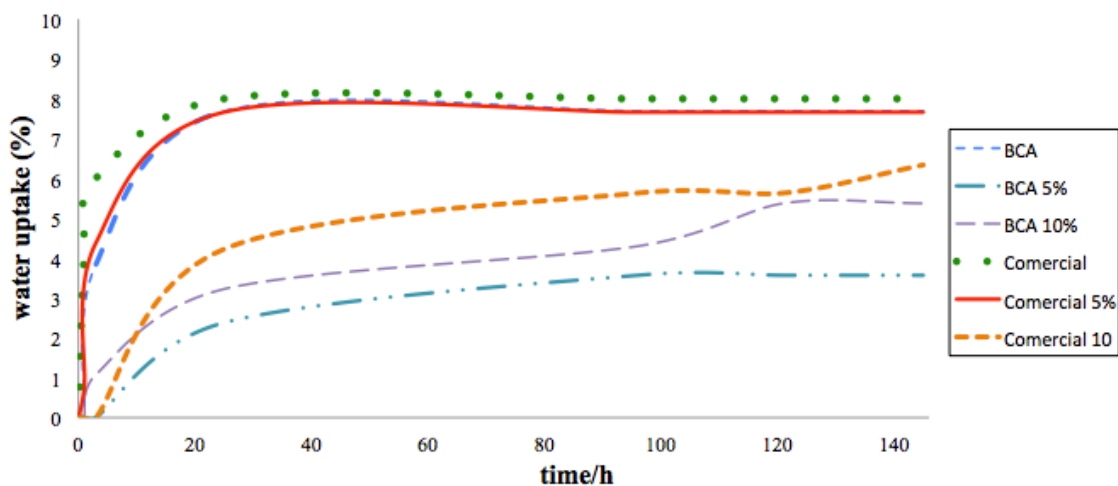
Figure 19. Water-uptake of the studied bacterial cellulose triacetate (BCA) and commercial cellulose triacetate films.

5.2.6. Photoluminescence and lifetime

5.2.6.1. Photoluminescence

The photoluminescence excitation and emission spectra of all the films containing BCA and commercial cellulose triacetate complexes of Tb^{3+} generally reveal that the ligand-lanthanide synergy is maintained after the addition.

The absence of the intra-$4f^8$ lines in the excitation spectra (Figure 21 and 22) is a proof of the efficiency of the ligand to absorb energy and transfer it to Tb^{3+} ions.

However, there exist some degrees of variations, from 1% and from 5% lanthanide complexes, in the disappearance of the BCA matrix band as can see in the excitation spectra on Figure 21a and 21b.

The photoluminescence maxima bands at 490, 545, 585 and 622 nm are attributed, respectively, to the $^5D_4 \rightarrow {}^7F_6$, $^5D_4 \rightarrow {}^7F_5$, $^5D_4 \rightarrow {}^7F_4$ and $^5D_4 \rightarrow {}^7F_3$, typical transitions of Tb^{3+} ions.[55]

The BCA (and commercial cellulose triacetate) composite films containing $Tb(acac)_3$ exhibit green emission under UV light (Figure 22).
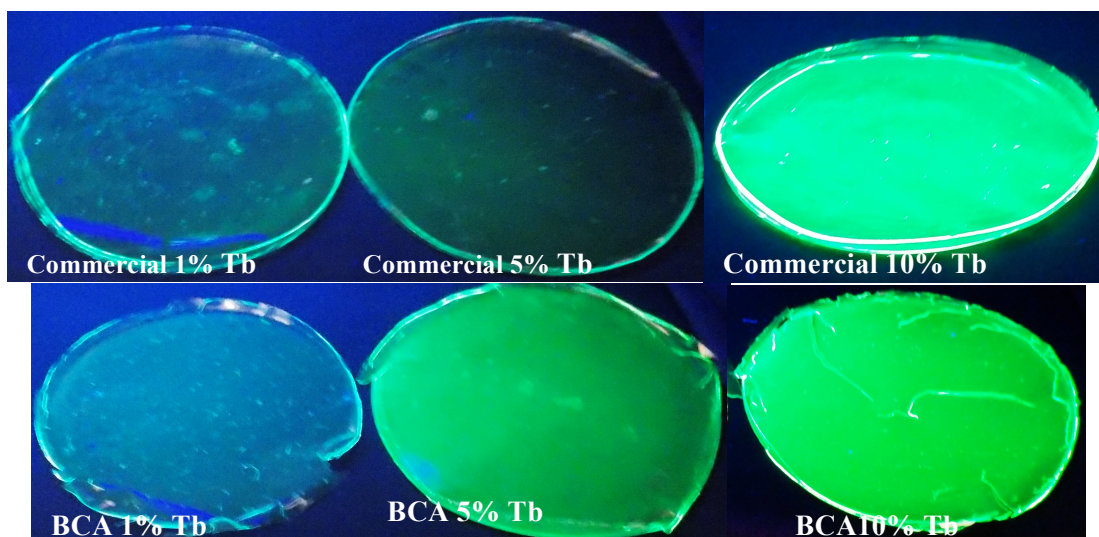
Figure 20. Photographs of BCA and commercial samples under UV light.
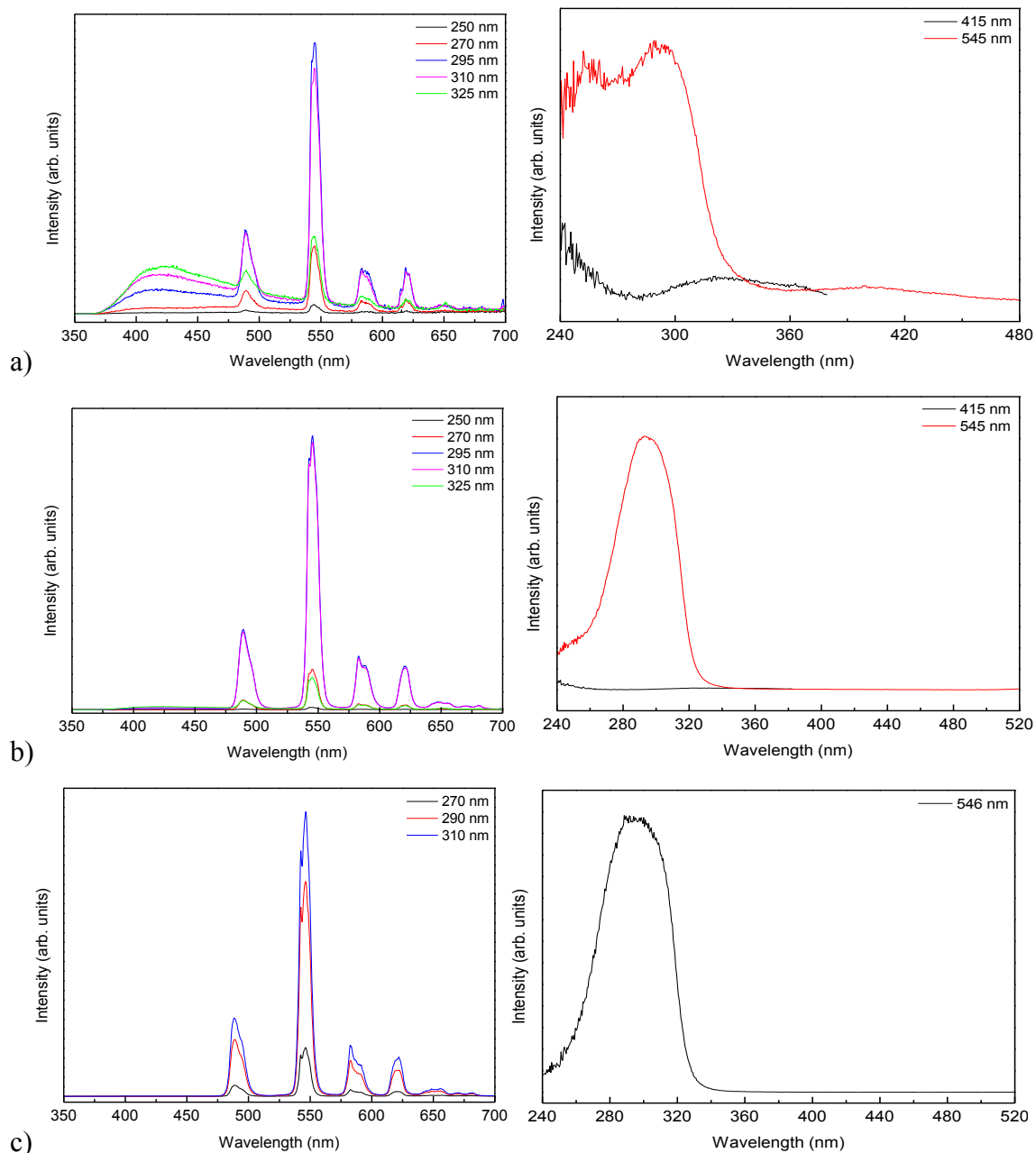
Figure 21. Emission (left) and excitation (right) spectra of BCA a) 1% Tb, b) 5% Tb, c) 10% Tb
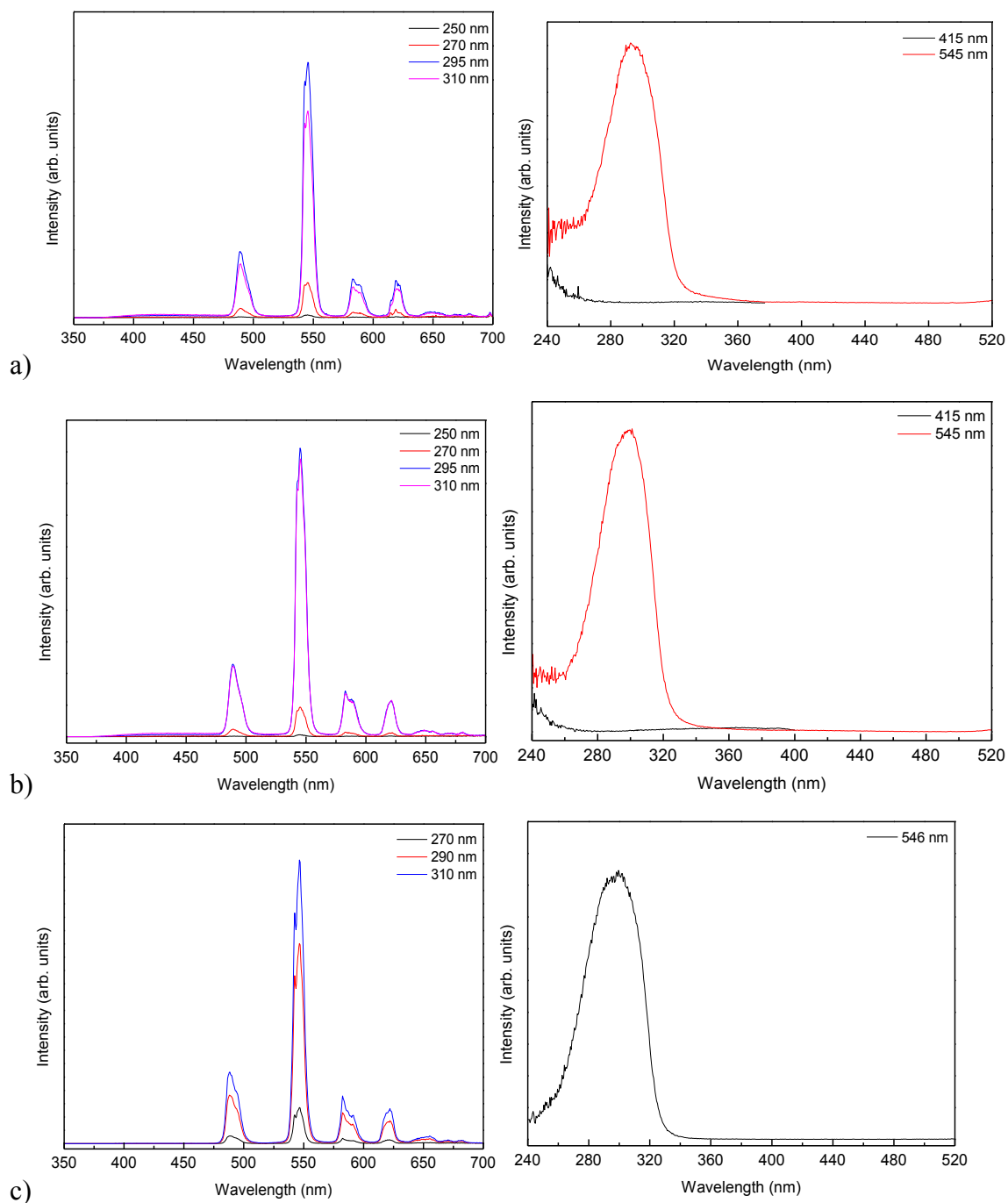
Figure 22. Emission (left) and excitation (right) spectra of commercial a) 1% Tb, b) 5% Tb, c) 10% Tb

5.2.6.2. Lifetime values

The lifetime of the excited states of the Ln^{3+} ions is defined as a sum of duration times of the ion intrinsic luminescence (radiative emission) and the non-radioactive deactivation processes.[11] The obtained $^5D_4$ lifetime values are listed in Table 5.

The increase of the $^5D_4$ lifetime values as the Tb^{3+} ($\tau_{Tb(acac)3}$= 0,774±0.001 ms [63]) amount increases in the films can be explained by an increase on the radiative emission due to the presence of more emitting centres.[78]

Table 5. $^5D_4$ lifetime values (ms) monitored at 545 nm under distinct excitation wavelengths (λ_{ex}, nm).

Reference	λ_{ex}	λ_{em}	τ (ms)(300 K)
BCA 1% Tb	295	545	0.737±0.006
BCA 5% Tb	295	545	0.819±0.002
BCA 10% Tb	290	546	1,067±0.003
	310		1,048±0.003
Comercial 1% Tb	295	545	0.628±0.005
Comercial 5% Tb	295	545	0.839±0.006
Comercial 10% Tb	290	546	0.995±0.002
	310		1,013±0.003

5.2.7. Emission quantum yields

The quantum yields of the terbium hybrids films of BCA and commercial cellulose triacetate are shown in Table 6.

Quantum yield is the ratio between the numbers of photons emitted and the number of photons absorbed.

As can be seen in Table 8, the greater values correspond to 10% concentration for both cellulose matrices, without a drastic difference on the emission quantum yields between them.

Table 6. Absolute emission quantum yields (ϕ) obtained at different excitation wavelengths (λ_{exc}, nm).

Reference	λ_{exc}	ϕ
BCA 1% Tb	250	<0.01
	275	
	295	0.02
BCA 5% Tb	250	<0.01
	275	
	295	0.09
BCA 10% Tb	275	0,11
	295	0,18
	310	0,20
Commercial 1% Tb	250	<0.01
	275	
	295	0.02
Commercial 5% Tb	250	<0.01
	275	0.04
	295	
Commercial 10% Tb	275	0,08
	295	0,18
	310	0,26

5.2.8. UV-Vis-NIR absorption spectra

As the trend in the other physical properties, the absorbance in the ultraviolet region is higher, when the luminescent agent amount increases.

While in the film of 10% the two samples display similar absorption, with a 1 and 5% of Tb^{3+} the difference between the absorption of commercial and bacterial cellulose is appreciable.
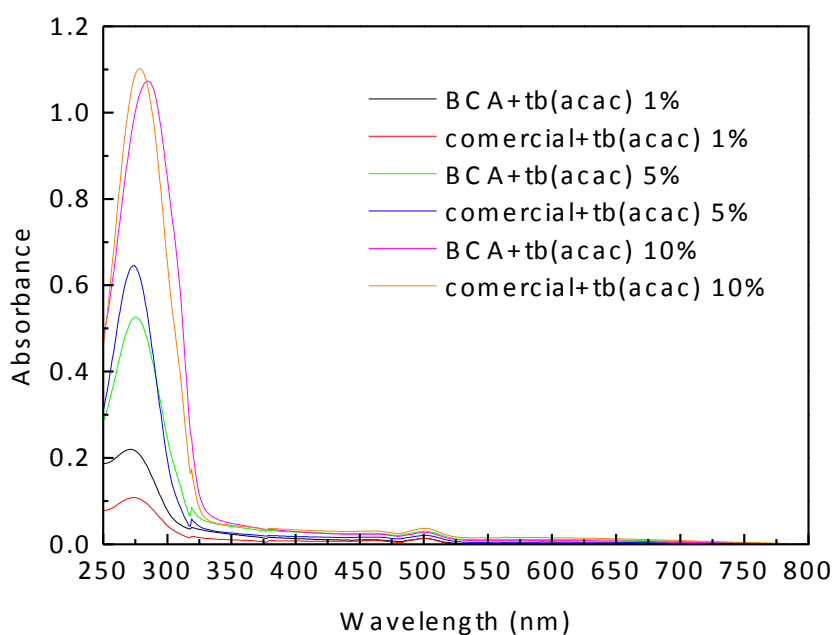
Figure 23. UV-Vis absorbance spectra of BCA 1% Tb, Commercial 1% Tb, BCA 5% Tb, Commercial 5% Tb, BCA 10% Tb, Commercial 10% Tb.

5.3. Partially acetylated bacterial cellulose films (preliminary study)

The use of bacterial cellulose nanofibers as reinforcing elements in composite materials had gained considerable interest in the last years. In this sense, aiming to produce BCA doped luminescent films with better mechanical properties; partial acetylated BC nanofibers were used as fillers in these films.

Bacterial cellulose nanofibers were partially acetylated with acetic anhydride, in presence of sulphuric acid, for 4h at 30°C. The schematic representation of BC partial acetylation is displayed in the Figure 24.
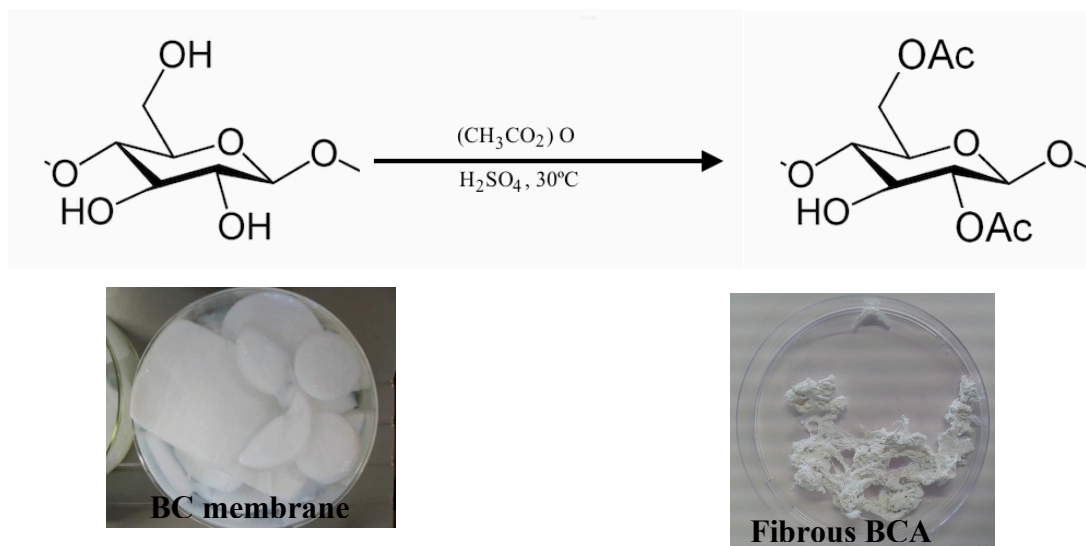
Figure 24. Schematic representation of the BCA partial acetylation and visual aspect of fibrous BCA before and after modification.

The occurrence of the partial acetylation reaction was primary confirmed based on the visible preservation of the BC nanofibers after reaction, however with a harder aspect. The success of the BC acetylation was further confirmed by FTIR (Figure 25), based on the appearance of the typical vibration of the acetate groups, previously described for the triacetate derivatives. The presence of the broad band typical of OH vibrations at 3500-3000 cm^{-1}, confirms the partial modification on the BC nanofibrils.
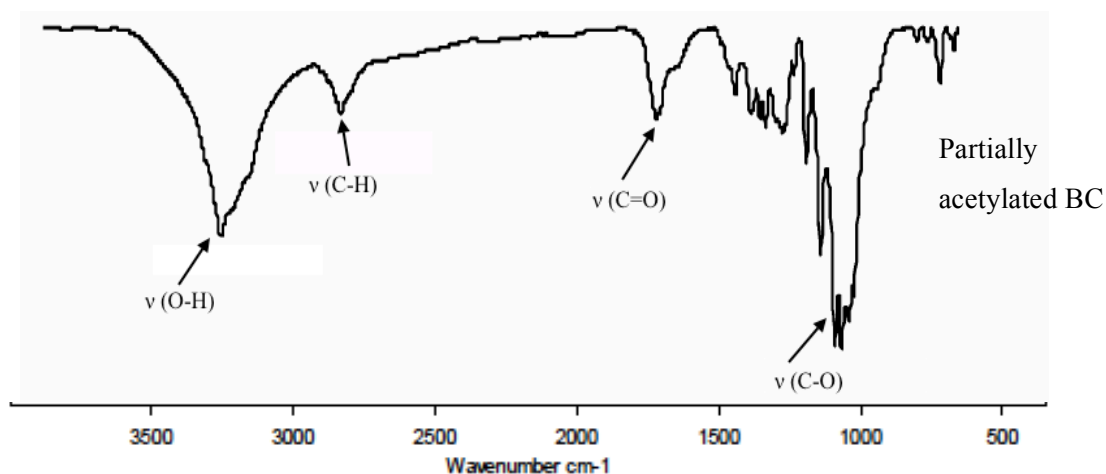
Figure 25. ATR- FTIR spectra of partially acetylated BC.

43

Then, the partially acetylated BC nanofibers were used as reinforcing elements (at 5 and 10% of load) in the BCA films doped with 5% of lanthanide complex. The obtained films were characterized by FTIR and mechanical and photophysical assays.

5.3.1. Fourier Transform Infrared Spectroscopy

The FTIR spectra of the BCA films doped with Tb(acac)$_3 \cdot 3$H$_2$O and reinforced with 5 and 10 % of partially acetylated BC showed also only the typical absorption bands of cellulose triacetate matrices described before. The typical vibrations of the partially acetylated BC nanofibers were not visible even for 10% of reinforcement.
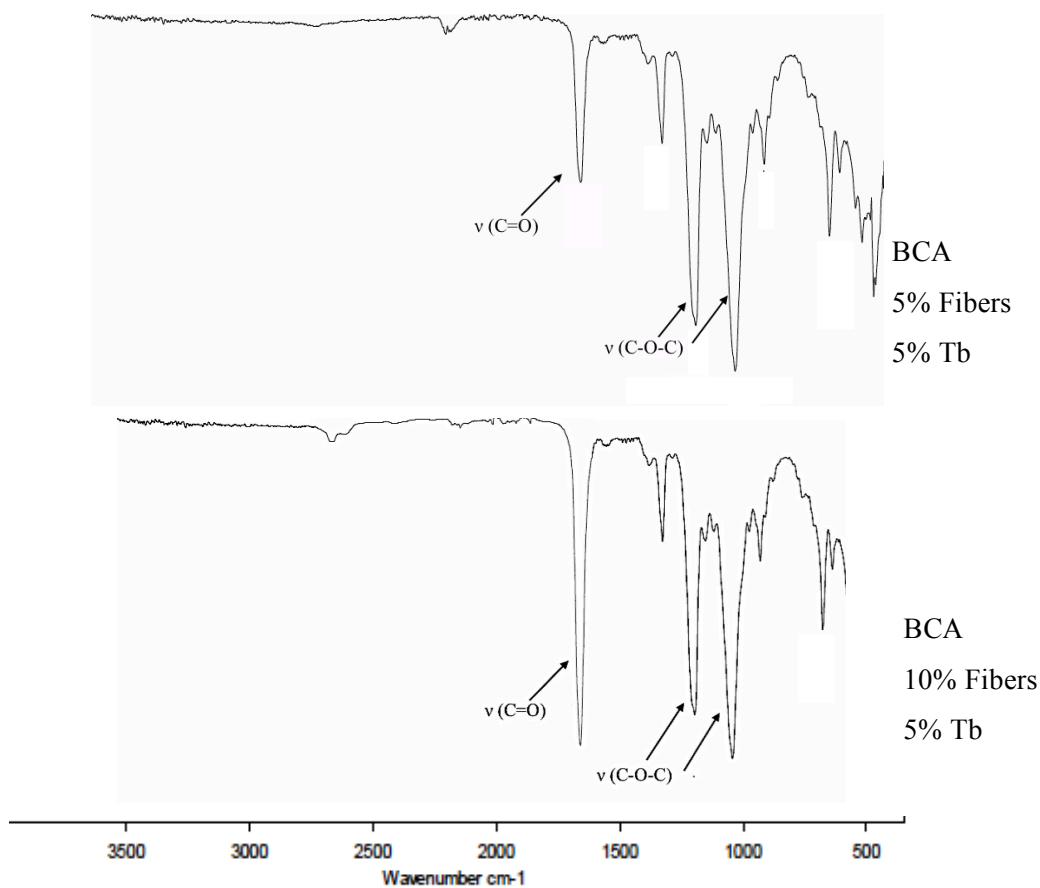
Figure 26. ATR- FTIR spectra of BCA+ 5% fibers + 5% Tb and BCA + 10% fibers + 5%Tb

5.3.2. Mechanical assays

The mechanical performance of the reinforced BCA films was also studied by tensile experiments (Figure 27).

As expected, the BCA doped films filled with the partially acetylated fibers are more rigid than their counterparts without fibers (Figure 18), as shown by the considerable increments on the Young modulus and the concomitant decrease of the elongation at break. The tensile strength was poorly affected by the addition of the partially acetylated BC nanofibers.
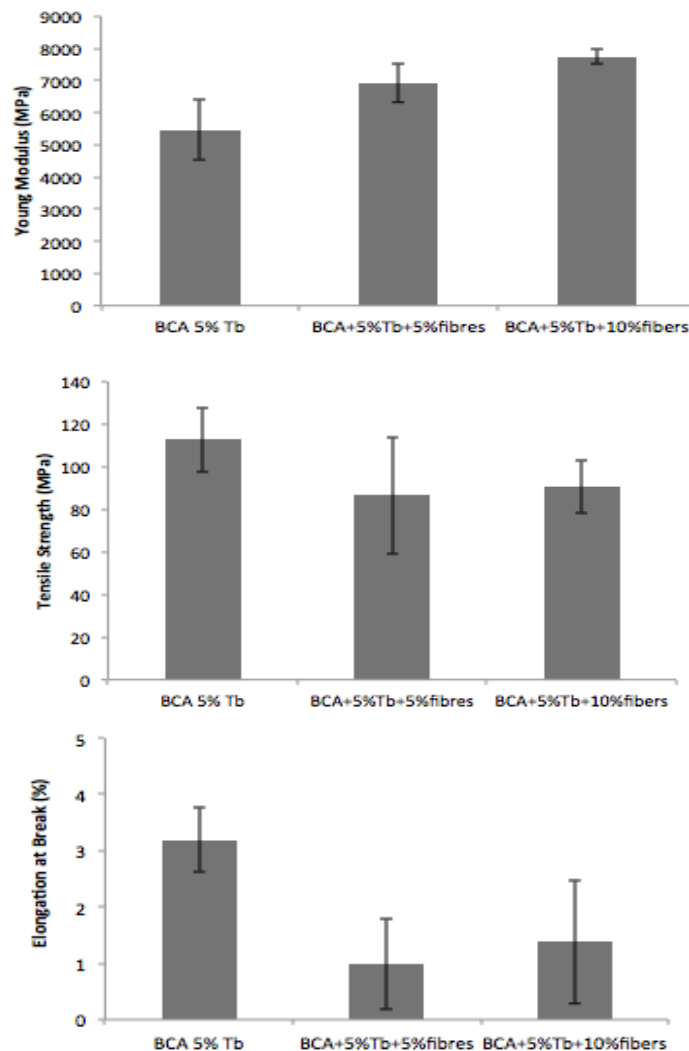
Figure 27. Young's modulus, tensile strength and elongation at break graphics of bacterial cellulose triacetate (BCA) with partially acetylated bacterial cellulose and with terbium complex.

Table 7. Young's modulus, tensile strength and elongation at break values of bacterial cellulose triacetate (BCA) and partially acetylated bacterial cellulose with 5% terbium complex.

Sample	Young Modulus (MPa)	Tensile Strength (MPa)	Elongation at Break (%)
BCA %5 fiber %5 Tb	6921,48±397,78	86,47±19,88	0,99±0,17
BCA 10% fiber %5 Tb	7746±430,55	90,85±15,79	1,39±0,871

5.3.3. Photoluminescence and lifetime

5.3.3.1. Photoluminescence

The photoluminescence spectrum of BCA and partially acetylated BC fibers films doped with 5% Tb(acac)$_3$ are shown at Figure 29 and 30.

The photoluminescence maxima bands at 490, 545, 585 and 622 nm are attributed, respectively, to the $^5D_4 \rightarrow {}^7F_6$, $^5D_4 \rightarrow {}^7F_5$, $^5D_4 \rightarrow {}^7F_4$ and $^5D_4 \rightarrow {}^7F_3$, typical transitions of Tb^{3+}. [55]

The BCA composite films containing Tb(acac)$_3$ exhibit green emission under UV light (Figure 28).
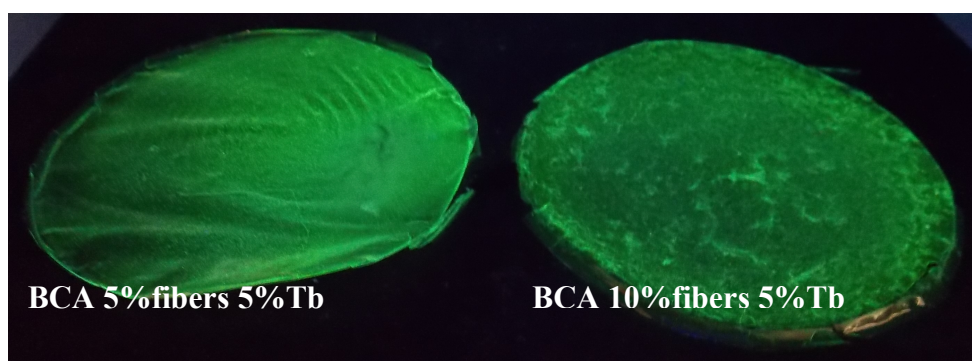
Figure 28. Photographs of BCA with partially acetylated bacterial cellulose samples under UV light.
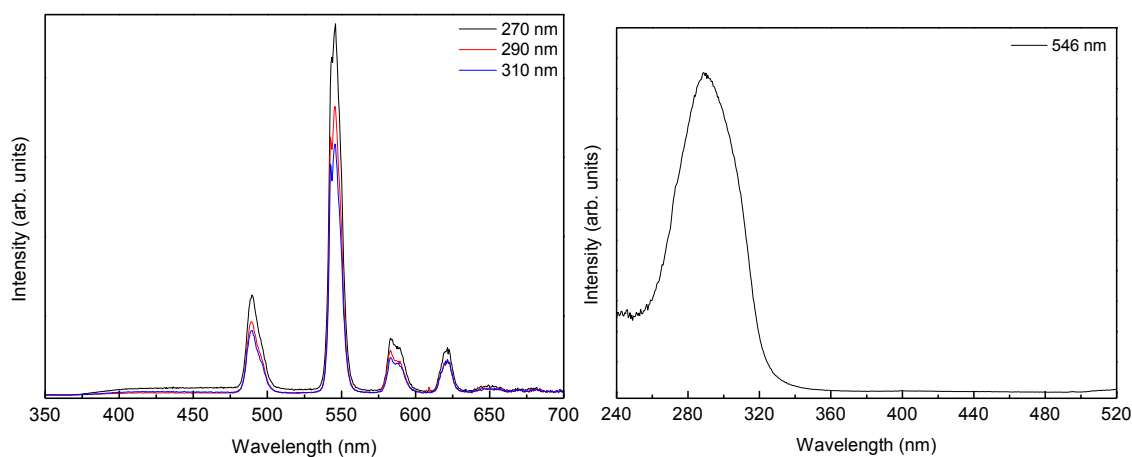
Figure 29. Emission (left) and excitation (right) spectra of BCA 5%fibres 5%Tb.
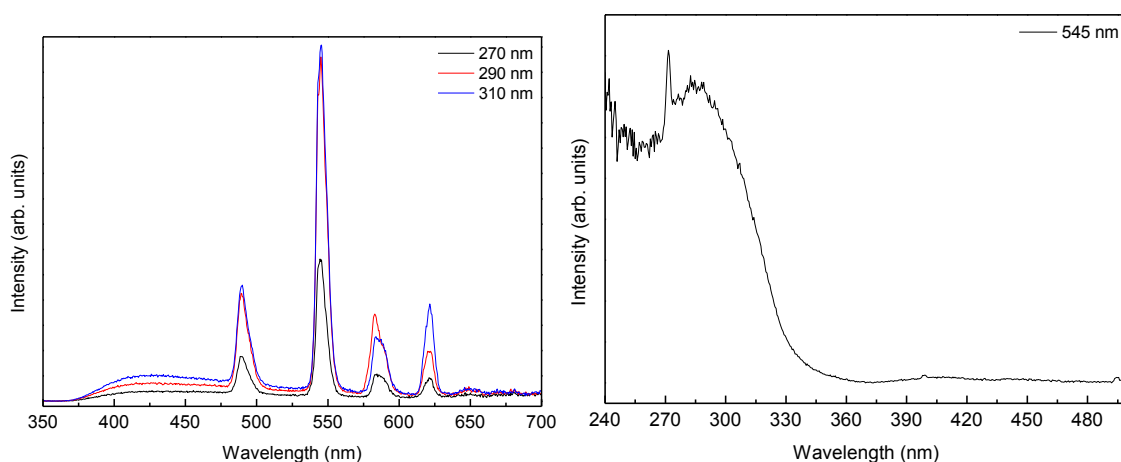
Figure 30. Emission (left) and excitation (right) spectra of BCA10% fibres 5%Tb.

5.3.3.2. Lifetime values

Both films of BCA and fibres with terbium ion show a decrease lifetime value compared with BCA and commercial cellulose triacetate films lifetime.

Table 8. $^5D_4$ lifetime values (ms) monitored at 545 nm under distinct excitation wavelengths (λ_{ex}, nm).

Reference	λ_{ex}	λ_{em}	τ (ms)(300 K)
BCA 5%fibres 5%Tb	290	546	0.649 ± 0.004
BCA 10% fibres 5%Tb	290	545	0.436 ± 0.008

5.3.4. Emission quantum yields

The incorporation of BCA fibers, as shown at lifetime values, affects the emission quantum yields, decreasing the value compared with the BCA samples with the same amount of terbium ($\phi_{\lambda exc =295}$=0,09).

Table 9. Absolute emission quantum yields (ϕ) obtained at different excitation wavelengths (λ_{exc}, nm).

Reference	λ_{exc}	ϕ
BCA 5%fibres 5%Tb	250	0.01
	275	0.03
	295	0.06
BCA 10%fibres 5%Tb	250	0.01
	275	0.02
	295	0.04

6. Conclusions

The present work described the successful preparation of novel luminescent films based on bacterial cellulose triacetate (BCA) (prepared by almost complete acetylation of bacterial cellulose, as confirmed by FTIR and ^{13}C NMR) and a terbium complex (Tb(acac)$_3$). The films were obtained by the simple dispersion of different amounts (1, 5 and 10%) of the lanthanide complex into a solution of cellulose acetate in dichloromethane, followed by solvent casting.

All the obtained films were very homogeneous and transparent, and displayed improved thermal and mechanical properties, as evidenced by reasonable increments in the maximum degradation temperature, and Young modulus and tensile strength, respectively. However, the films with 5% of Tb(acac)$_3$ showed the better results.

In addition, as expected, the increment of lanthanide quantity in the films, due to the presence of more emitting centres, improved the luminescent properties, such as, lifetime and emission quantum yields values.

Preliminary results on the addition of partially acetylated bacterial cellulose to the lanthanide loaded films resulted in considerable increments on the Young modulus (increasing 42%), without compromising in a great extent their photoluminescent properties.

Finally, future research activities to continue and complement this study will consider the following issues:

- The combination of cellulose triacetates with other complexes that increase the antenna effect aiming to enhance the luminescence.
- The improvement of the mechanical properties of the films by addition of partial acetylated cellulose nanofibers (or other reinforcing elements) with different DS values.
- The processing of the materials with other forms or morphologies, for example by electrospinning.
- The search for greener alternatives for the processing of the materials, i.e. avoiding the use of harmful organic solvents.

7. Bibliography

1. Gandini, A. Polymers from Renewable Resources: A Challenge for the Future of Macromolecular Materials. *Macromolecules* **2008**, *41*, 9491–9504.

2. Huber, T.; Müssig, J.; Curnow, O.; Pang, S.; Bickerton, S.; Staiger, M. P. A critical review of all-cellulose composites. *J. Mater. Sci.* **2012**, *47*, 1171–1186.

3. Weili Hu, S. C. Solvent-free acetylation of bacterial cellulose under moderate conditions. *Carbohydr. Polym.* **2011,83,** 1575–1581.

4. Freire, C. S. R.; Fernandes, S. C. M.; Silvestre, A. J. D.; Neto, C. P. Novel cellulose-based composites based on nanofibrillated plant and bacterial cellulose: recent advances at the University of Aveiro – a review. *Holzforschung* **2012**, *0*, 1–10.

5. Pinto, R. J. B.; Granadeiro, C. M.; Freire, C. S. R.; Silvestre, A. J. D.; Neto, C. P.; Ferreira, R. A. S.; Carlos, L. D.; Cavaleiro, A. M. V.; Trindade, T.; Nogueira, H. I. S. Luminescent Transparent Composite Films Based on Lanthanopolyoxometalates and Filmogenic Polysaccharides. *Eur. J. Inorg. Chem.* **2013**, *2013*, 1890-1896.

6. Zhang, C.; Lin, J. Defect-related luminescent materials: synthesis, emission properties and applications. *Chem. Soc. Rev.* **2012**, *41*, 7938-7961.

7. Azevedo, C. B. Optical properties of Eu-doped hybrid materials prepared from dimethyl and methyl alkoxides precursors. *J. Lumin.* **2013**, *134*, 551–557.

8. Meshkova, S. B. The Dependence of the Luminescence Intensity of Lanthanide Complexes with β-Diketones on the Ligand Form. *J. Fluoresc.* **2000**, *10*, 333–337.

9. Hanna, A. A.; Basta, A. H.; El-Saied, H.; Abadir, I. F. Thermal properties of cellulose acetate and its complexes with some transition metals. *Angew. Makromol. Chem.* **1998**, *260*, 1–4.

10. Zhou, Z.; Wang, Q. Two emissive cellulose hydrogels for detection of nitrite using terbium luminescence. *Sens. Actuators B Chem.* **2012**, *173*, 833–838.

11. Vázquez-Guilló, R., Calero, A., Valente, A. J. M., Burrows, H. D., Reyes Mateo, C., Mallavia, R., *Novel electrospun luminescent nanofibers from cationic polyfluorene/cellulose acetate blend* - Springer, **2013**, *20,* 169-177

12. Kamide, K. *Cellulose and Cellulose Derivatives*; First edition.; Elsevier: Amsterdam, The Netherlands, 2005.

13. Anselme Payen Biography [Internet] Available from: http://chemistry.about.com/od/famouschemists/p/anselme-payen-bio.htm (accessed Mar

11, 2013).

14. Zugenmaier, P. *Crystalline Cellulose and Cellulose Derivatives: Characterization and Structures*; Springer: New York, 2008.

15. Wertz, J. L.; Bédué, O.; Mercier, J. P. *Cellulose Science and Technology*; First edition.; EPFL Press: Switzerland, 2010.

16. Nomenclature of Carbohydrates [Internet] Available from: *http://www.chem.qmul.ac.uk/iupac/2carb/25n26.html*.

17. Jonas, R.; Farah, L. F. Production and application of microbial cellulose. *Polym. Degrad. Stab.* **1998**, *59*, 101–106.

18. Lewin, M. *Handbook of Fiber Chemistry.*; Third edition.; CRC Press: Boca Ratón, United State of America, 2010.

19. Dufresne, A. *Nanocellulose: From Nature to High Performance Tailored Materials*; First edition.; Walter de Gruyter: France, 2012.

20. Kaith, B. S. *Cellulose Fibers: Bio- and Nano-Polymer Composites: Green Chemistry and Technology*; First edition.; Springer: Heidelberg, 2011.

21. Müssig, J. *Industrial Applications of Natural Fibres: Structure, Properties and Technical Applications*; First edition.; John Wiley & Sons: United Kingdom, 2010.

22. Fischer, S.; Thümmler, K.; Volkert, B.; Hettrich, K.; Schmidt, I.; Fischer, K. Properties and Applications of Cellulose Acetate. *Macromol. Symp.* **2008**, *262*, 89–96.

23. Coleman, J. N.; Khan, U.; Gun'ko, Y. K. Mechanical Reinforcement of Polymers Using Carbon Nanotubes. *Adv. Mater.* **2006**, *18*, 689–706.

23. Biopolymers book, Vol.6: Plysaccharides II: Polysaccharides from Eukaryotes [Internet] Available from: www.wiley-vch.de/books/biopoly/pdf_v06/bpol6010_275_287.pdf.

25. Shmulsky, R.; Jones, P. D. *Forest Products and Wood Science*; Sixth edition.; John Wiley & Sons: Oxford, 2011.

26. Eichhorn, S. J.; Dufresne, A.; Aranguren, M.; Marcovich, N. E.; Capadona, J. R.; Rowan, S. J.; Weder, C.; Thielemans, W.; Roman, M.; Renneckar, S.; Gindl, W.; Veigel, S.; Keckes, J.; Yano, H.; Abe, K.; Nogi, M.; Nakagaito, A. N.; Mangalam, A.; Simonsen, J.; Benight, A. S.; Bismarck, A.; Berglund, L. A.; Peijs, T. Review: current international research into cellulose nanofibres and nanocomposites. *J. Mater. Sci.* **2010**, *45*, 1–33.

27. CCI Notes 13/11 http://www.cci-icc.gc.ca/publications/notes/13-11-eng.aspx

(accessed Jul 18, 2013).

28. Sjöström, E. *Wood Chemistry: Fundamentals and Applications*; Second editions.; Gulf Professional Publishing: California, United States of America, 1993.

29. Brown, R. M.; Willison, J. H.; Richardson, C. L. Cellulose biosynthesis in Acetobacter xylinum: visualization of the site of synthesis and direct measurement of the in vivo process. *Proc. Natl. Acad. Sci.* **1976**, *73*, 4565–4569.

29. Biopolymers book, Vol.5: Plysaccharides I: Polysaccharides from Prokaryotes [Internet] Available from: www.wiley-vch.de/books/biopoly/pdf_v05/bpol5003_37_46.pdf.

31. Watanabe, K.; Tabuchi, M.; Morinaga, Y.; Yoshinaga, F. Structural Features and Properties of Bacterial Cellulose Produced in Agitated Culture. *Cellulose* **1998**, *5*, 187–200.

32. Ifuku, S.; Nogi, M.; Abe, K.; Handa, K.; Nakatsubo, F.; Yano, H. Surface Modification of Bacterial Cellulose Nanofibers for Property Enhancement of Optically Transparent Composites: Dependence on Acetyl-Group DS. *Biomacromolecules* **2007**, *8*, 1973–1978.

33. Eichhorn, S. J.; Baillie, C. A.; Zafeiropoulos, N.; Mwaikambo, L. Y.; Ansell, M. P.; Dufresne, A.; Entwistle, K. M.; Herrera-Franco, P. J.; Escamilla, G. C.; Groom, L.; Hughes, M.; Hill, C.; Rials, T. G.; Wild, P. M. Review: Current international research into cellulosic fibres and composites. *J. Mater. Sci.* **2001**, *36*, 2107–2131.

34. M., M.-N.; R., Y., A. Investigation of Physicochemical Properties of the Bacterial Cellulose Produced by Gluconacetobacter xylinus from Date Syrup. *World Academy of Science, Engineering and Technology* **2010**, *44*, 1258–1263.

35. Maneerung, T.; Tokura, S.; Rujiravanit, R. Impregnation of silver nanoparticles into bacterial cellulose for antimicrobial wound dressing. *Carbohydr. Polym.* **2008**, *72*, 43–51.

36. Pacheco, J. L. C.-; Yee, S. M.; Zentella, M. C.; Marván, E. E. Celulosa bacteriana en gluconacetobacter xylinum: biosíntesis y aplicaciones. *Tip Rev. Espec. En Cienc. Quím.-Biológicas* **2004**, *7*, 18–25.

37. Klemm, D.; Heublein, B.; Fink, H.-P.; Bohn, A. Cellulose: fascinating biopolymer and sustainable raw material. *Angew. Chem. Int. Ed Engl.* **2005**, *44*, 3358–3393.

38. Paul Schützenberger Acide acétique - Action de l'acide acétique anhydre sur la cellulose, les sucres, la mannite et ses congénères. *Comptes Rendus Chim.* **1865**, *61*,

485–486.

39. Shah, J.; Jr, R. M. B. Towards electronic paper displays made from microbial cellulose. *Appl. Microbiol. Biotechnol.* **2005**, *66*, 352–355.

40. Heterogeneous process for acetylation of celluloses [Internet] Available from: *http://pac.iupac.org/publications/pac/pdf/1967/pdf/1403x0507.pdf*.

41. Cellulose Acetate [Internet] Available from: *www.azom.com/article.aspx?ArticleID=1461*.

42. Tsioptsias, C.; Sakellariou, K. G.; Tsivintzelis, I.; Papadopoulou, L.; Panayiotou, C. Preparation and characterization of cellulose acetate–Fe2O3 composite nanofibrous materials. *Carbohydr. Polym.* **2010**, *81*, 925–930.

43. Yu, L. *Biodegradable Polymer Blends and Composites from Renewable Resources*; John Wiley & Sons: New Jersey, 2009.

44. Bheda, J.; Fellers, J. F.; White, J. L. Wet spinning of liquid crystalline solutions of cellulose acetate butyrate and cellulose triacetate. *J. Appl. Polym. Sci.* **1981**, *26*, 3955–3961.

45. Buchanan, C. M.; Gardner, R. M.; Komarek, R. J. Aerobic biodegradation of cellulose acetate. *J. Appl. Polym. Sci.* **1993**, *47*, 1709–1719.

46. Seoud, O. A. E.; Heinze, T. Organic Esters of Cellulose: New Perspectives for Old Polymers. In *Polysaccharides I*; Heinze, T., Ed.; Advances in Polymer Science; Springer Berlin Heidelberg, 2005; pp. 103–149.

47. Yilu Guo; Peiyi Wu Investigation of the hydrogen-bond structure of cellulose diacetate two-dimensional infrared correlation spectroscopy. *Carbohydr. Polym.* **2008**, *74*, 509–513.

48. Volodymyr Kuzmenko Carbon nanofibers synthesized from electrospun cellulose. Master of Science Thesis in Materials and Nanotechnology, CHALMERS UNIVERSITY OF TECHNOLOGY.

49. Singh, G. *Chemistry Of Lanthanides And Actinides*; First edition.; Discovery Publishing House: India, 2007.

50. Sathyanarayana, D. N. *Electronic Absorption Spectroscopy and Related Techniques*; First edition.; Universities Press: India, 2001.

51. Nomenclature of Inorganic Chemistry-IUPAC [Internet] Available from: *www.iupac.org/publications/books/rbook/Red_Book_2005.pdf*.

52. Hänninen, P. *Lanthanide Luminescence: Photophysical, Analytical and Biological*

Aspects; First edition.; Springer: Heidelberg, 2011.

53. Martinus H.V. Werts Making Sense of Lanthanide Luminescence. *Sci. Prog.* **2005**, *88(2)*, 101–131.

54. Chawla, P. R.; Bajaj, I. B.; Survase, S. A.; Singhal, R. S. Microbial Cellulose: Fermentative Production and Applications. *Food Technol. Biotechnol.* **2009**, *47*, 107–124.

55. *Functional Hybrid Materials*; Gómez-Romero, P.; Sanchez, C., Eds.; First edition.; John Wiley & Sons, 2006.

56. Kickelbick, G. *Hybrid Materials: Synthesis, Characterization, and Applications*; John Wiley & Sons, 2007.

57. Wang, M.; Abbineni, G.; Clevenger, A.; Mao, C.; Xu, S. Upconversion nanoparticles: synthesis, surface modification and biological applications. *Nanomedicine Nanotechnol. Biol. Med.* **2011**, *7*, 710–729.

58. Chung, J. H. Effect of Yb3 and Tm3 concentrations on blue and NIR upconversion luminescence in Yb3 , Tm3 co-doped CaMoO4. *Ceram. Int.* **2013**, *39*, 1951–1956.

59. Wang, F.; Liu, X. Recent advances in the chemistry of lanthanide-doped upconversion nanocrystals. *Chem. Soc. Rev.* **2009**, *38*, 976–989.

60. National Science Fundation, a Colorful Approach to Solar Energy. [Internet] Available from: *www.nsf.gov/news/news_images.jsp?cntn_id=111903&org=NSF*.

61. Gaponenko, N. V.; Sergeev, O. V.; Borisenko, V. E.; Pivin, J. C.; Skeldon, P.; Thompson, G. E.; Hamilton, B.; Misiewicz, J.; Bryja, L.; Kudrawiec, R.; Stupak, A. P.; Stepanova, E. A. Terbium photoluminescence in polysiloxane films. *Mater. Sci. Eng. B* **2001**, *81*, 191–193.

62. Trovatti, E.; Serafim, L. S.; Freire, C. S. R.; Silvestre, A. J. D.; Neto, C. P. Gluconacetobacter sacchari: An efficient bacterial cellulose cell-factory. *Carbohydr. Polym.* **2011**, *86*, 1417–1420.

63. Lima, P. P.; Ferreira, R. A. S.; Júnior, S. A.; Malta, O. L.; Carlos, L. D. Terbium(III)-containing organic–inorganic hybrids synthesized through hydrochloric acid catalysis. *J. Photochem. Photobiol. Chem.* **2009**, *201*, 214–221.

64. Sassi, J.-F.; Chanzy, H. Ultrastructural aspects of the acetylation of. *Cellulose* **1995**, *2*, 111–127.

65. Tomé, L. C.; Pinto, R. J. B.; Trovatti, E.; Freire, C. S. R.; Silvestre, A. J. D.; Neto, C. P.; Gandini, A. Transparent bionanocomposites with improved properties prepared

from acetylated bacterial cellulose and poly(lactic acid) through a simple approach. *Green Chem.* **2011**, *13*, 419–427.

66. Barud, H. S.; Souza, J. L.; Santos, D. B.; Crespi, M. S.; Ribeiro, C. A.; Messaddeq, Y.; Ribeiro, S. J. L. Bacterial cellulose/poly(3-hydroxybutyrate) composite membranes. *Carbohydr. Polym.* **2011**, *83*, 1279–1284.

67. Lima, G. de M.; Sierakowski, M.-R.; Faria-Tischer, P. C. S.; Tischer, C. A. Characterisation of bacterial cellulose partly acetylated by dimethylacetamide/lithium chloride. *Mater. Sci. Eng. C* **2011**, *31*, 190–197.

68. Mohd Edeerozey Abd Manaf; Manami Tsuji; Shogo Nobukawa; Masayuki Yamaguchi Effect of Moisture on the Orientation Birefringence of Cellulose Esters. *Polymers* **2011**, *3*, 955–966.

69. Isogai, A. NMR analysis of cellulose dissolved in aqueous NaOH solutions. *Cellulose* **1997**, *4*, 99–107.

70. Cerqueira, D. A.; Rodrigues Filho, G.; Carvalho, R. de A.; Valente, A. J. M. 1H-NMR characterization of cellulose acetate obtained from sugarcane bagasse. *Polímeros* **2010**, *20*, 85–91.

71. VanderHart, D. L.; Hyatt, J. A.; Atalla, R. H.; Tirumalai, V. C. Solid-State 13C NMR and Raman Studies of Cellulose Triacetate: Oligomers, Polymorphism, and Inferences about Chain Polarity. *Macromolecules* **1996**, *29*, 730–739.

72. Kobayashi, H.; Ito, Y.; Komanoya, T.; Hosaka, Y.; Dhepe, P. L.; Kasai, K.; Hara, K.; Fukuoka, A. Synthesis of sugar alcohols by hydrolytic hydrogenation of cellulose over supported metal catalysts. *Green Chem.* **2011**, *13*, 326–333.

73. Kono, H.; Erata, T.; Takai, M. CP/MAS 13C NMR Study of Cellulose and Cellulose Derivatives. 2. Complete Assignment of the 13C Resonance for the Ring Carbons of Cellulose Triacetate Polymorphs. *J. Am. Chem. Soc.* **2002**, *124*, 7512–7518.

74. Barud, H. S.; Barrios, C.; Regiani, T.; Marques, R. F. C.; Verelst, M.; Dexpert-Ghys, J.; Messaddeq, Y.; Ribeiro, S. J. L. Self-supported silver nanoparticles containing bacterial cellulose membranes. *Mater. Sci. Eng. C* **2008**, *28*, 515–518.

75. VanderHart, D. L.; Hyatt, J. A.; Atalla, R. H.; Tirumalai, V. C. Solid-State 13C NMR and Raman Studies of Cellulose Triacetate: Oligomers, Polymorphism, and Inferences about Chain Polarity. *Macromolecules* **1996**, *29*, 730–739.

76. Sievers, R. *Nuclear Magnetic Resonance Shift Reagents*; Elsevier Science: New York, 2012.

77. Binnemans, K. Rare-earth beta-diketonates. In *Handbook on the Physics and Chemistry of Rare Earths*; K.A. Gschneidner, J.-C. B. and V. K. P., Ed.; Elsevier: Amsterdam, The Netherlands, 2005; Vol. Volume 35, pp. 107–272.

78. Salas, I. I. R.; Castolo, A. A. Resonancia magnética nuclear de compuestos paramagnéticos. *Educ. Quím. 8*, 4.

79. Jing Li; Li-Ping Zhang; Feng Peng; Jing Bian; Tong-Qi Yuan; Feng Xu; Run-Can Sun Microwave-assisted solvent-free acetylation of cellulose with acetic anhydride in the presence of iodine as catalyst. *Molecules* **2009**, *14*, 3551–3566.

80. Omar Arous; Mourad Amara; Hacène Kerdjoudj Selective transport of metal ions using polymer inclusion membranes containing crown ethers and cryptands. *AJSE-Egineering 35*.

81. Duclerc F. Parra; Hermi F. Brito; Luis D. Carlos Enhancement of the luminescent intensity of the novel system containing Eu3+-β-diketonate complex doped in the epoxy resin. *J. Appl. Polym. Sci.* **2002**, *83*, 2716–2726.

82. Jiang Kai; Maria C. F. C. Felinto; Luiz A. O. Nunes; Oscar L. Malta; Hermi F. Brito Intermolecular energy transfer and photostability of luminescence-tuneable multicolour PMMA films doped with lanthanide–β-diketonate complexes. *J. Mater. Chem.* **2011**, *21*, 3796–3802.

83. Bian, L.-J.; Qian, X.-F.; Yin, J.; Zhu, Z.-K.; Lu, Q.-H. Eu3+ complex/polyimide nanocomposites: Improvement in mechanical and thermal properties. *J. Appl. Polym. Sci.* **2002**, *86*, 2707–2712.